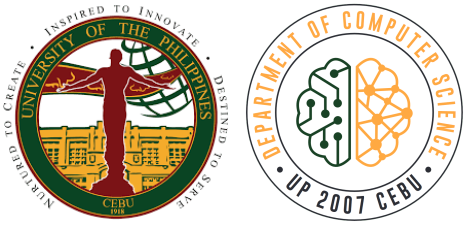

Development of a Finger-Key Identification Module for a Touch Typing Trainer

---

A Special Project Presented to the

Faculty of the Department of Computer Science,

University of the Philippines Cebu

In Partial Fulfillment

Of the Requirements for the Degree

Bachelor of Science in Computer Science

Oscar Vian L. Valles

BS Computer Science

Dhong Fhel K. Gom-os

Adviser

June 2022

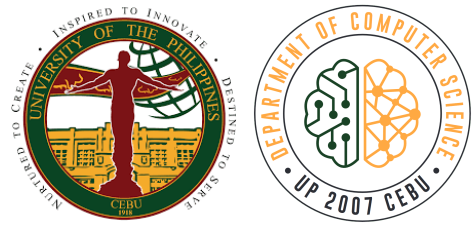

UNIVERSITY OF THE PHILIPPINES CEBU

College of Science

Department of Computer Science

DEVELOPMENT OF A FINGER-KEY IDENTIFICATION MODULE FOR A TOUCH TYPING TRAINER

Permission is given for the following people to have access to this thesis:

Available to the general public	Yes
Available only after consultation with author or thesis adviser	Yes
Available to those bound by confidentiality agreement	Yes

Oscar Vian L. Valles

Student

Dhong Fhel K. Gom-os

Special Problem Adviser

APPROVAL SHEET

The faculty of the University of the Philippines Cebu, College of Science, Department of Computer Science approves this Special Problem entitled:

Development of a Finger-Key Identification Module
for a Touch Typing Trainer

by

Oscar Vian L. Valles

Dhong Fhel K. Gom-os	Prof. Aileen Joan O. Vicente
Special Problem Adviser	Chair, Department of Computer Science
Date Signed	Date Signed

Prof. Nelia S. Ereno

Dean, College of Science

Date Signed

Abstract

Typing tests list out words for the user to repeat. These tests measure metrics that quantify the user's ability to type. However, conventional typing metrics do not measure correct finger placement. This aspect of typing may affect the user's health. It is also a crucial aspect of keyboard typing education. As such, a method to identify which finger is used to press which key is beneficial. This paper introduces a technique to achieve this by developing a finger-key identification module that utilizes computer vision algorithms to detect the keys in a keyboard, and a ready-made machine learning solution to track fingers while typing. This module was successful in finger-key identification with an accuracy of 99.58% in a dataset of 938 keypresses. The module also had an average finger-key identification time of 0.083 seconds, which allows the module to perform real-time finger-key identification for typing speeds up to 143.030 Words per Minute which is well beyond the median typing speed of the population. Furthermore, two metrics for correct finger placement were defined and were implemented in a proof-of-concept trainer: (1) Finger Placement Accuracy which computes the number of keys pressed using the correct finger in a typing test sequence, and (2) Historical Finger Placement Accuracy which evaluates the user's ability to press a certain key with the correct finger over multiple typing test sequences.

Acronyms

ANSI American National Standards Institute

CPS Characters per Second

CTS Carpal Tunnel Syndrome

FP ACC Finger Placement Accuracy

HFP ACC Historical Finger Placement Accuracy

ISO International Organization for Standardization

JIS Japanese International Standards

ROI Region of Interest

WPM Words per Minute

WRNULD Work-related neck and upper limb disorders

List of Tables

List of Figures

List of Equations

Table of Contents

Chapter 1

Introduction

1.1 Background of the Study

There are a lot of educational typing tests available that help people learn touch typing, including Monkeytype, TypeRacer, and Keybr. These typing tests list out words that are then typed out. The entered keys are then compared to check if the user has typed the expected letter. At the end of the test, the time taken is calculated, and certain metrics are given. These metrics include Words per Minute (WPM) and Accuracy (Arif & Stuerzlinger, 2009). However, this method of examination leaves out a crucial part of typing — correct finger placement.

Incorrect finger placement may affect hand and finger health. Incorrect placement of the fingers may cause these hand and wrist positions: ulnar deviation, forearm pronation, and wrist extension (Serina et al., 1999). These three are hand and wrist positions that are common in all activities, however, prolonged periods in these positions, such as in typing, may cause injuries such as Carpal Tunnel Syndrome (CTS) (Toosi et al., 2015).

Correct finger placement is usually taught at the beginning using a diagram, with each key being associated with a specific finger. For instance, the letter Q in a QWERTY layout should be pressed using the fifth digit, or the little finger, of the left hand, and this is shown on instruction manuals by coloring the fifth digit and the key Q with the same color or by placing the letters directly on the fingers (Dobson, 2009).

Furthermore, touch typing using correct finger placement is frequently taught in the beginner level (Donica et al., 2018). This means that there is a need to weed out bad habits that may develop,

like using the index finger for pressing the spacebar or backspace. However, it is impractical for an educator to check each student if they are not performing these movements as these may only show for a small period and may not be caught in time.

Thus, there is a need for automatically identifying which finger is used to press which key during typing — hereby defined as finger-key identification.

1.2 Research Questions

1. What algorithm or technique using computer vision is capable of finger-key identification.
2. What is the setup and configuration of a single optical camera can be used to capture images during keyboard typing for real-time finger-key identification using the algorithm identified in 1?
3. How to design and develop a finger-key identification module using the algorithm in 1 and camera setup and configuration in 2?
4. How accurate is the module developed in 3 in finger-key identification?
5. Is the module developed in 3 fast enough to run in real-time?
6. What new keyboard typing metric to develop that considers both the key and finger used to press as parameters?

1.3 Research Objectives

1.3.1 General Objectives

To create a finger-key identification module that accurately identifies what finger was used to press a key at a point in time to help develop better typing habits and healthier typing ergonomics.

1.3.2 Specific Objectives

1. Develop an algorithm or technique using computer vision capable of finger-key identification.
2. Identify the setup and configuration of a single optical camera that can be used to capture images during keyboard typing for finger-key identification using the algorithm identified in 1
3. Design and develop a module using the algorithm in 1 and camera setup and configuration in 2
4. Determine the accuracy of the module developed in 3 in finger-key identification
5. Determine if the module developed in 3 is fast enough to run in real-time
6. Develop a new keyboard typing metric that uses both the key and finger used to press as parameters

1.4 Scope and Limitation

The experimental setup was simplified and tightly controlled. It was not representative of real-world conditions. The colors of the keyboard, cables, and surface were all controlled. So were the lighting and camera used.

The supported keyboard of the module was limited to one specific type of keyboard. A 60% Keyboard in a slightly modified American National Standards Institute (ANSI) layout with light-colored keys was used as shown in Figure 1.1. This type of keyboard only has the alphanumeric portion of a full-size keyboard. This limited the number of keys to be checked and reduced the overall movement of the hand during typing. The keyboard layout was a slightly modified ANSI layout. The majority of the layout still followed the base ANSI layout, with the alphanumeric portion remaining exactly the same.

The module's effect on typing was not tested. This includes the module's effect on typing in education and typing in health, as the focus of the research was on the development and testing of the finger-key identification module only.

Figure 1.1: A 60% keyboard in ANSI layout.

1.5 Significance of the Research

This research is beneficial for all users of physical keyboards. These include a majority of the population as there are a lot of professions that heavily rely on keyboards. Examples include developers, physicians, educators, and accountants. By having better ergonomics while typing — by touch typing correctly — wrist injuries can be prevented, and typing speed may be increased.

This research also helps educators, especially early educators teaching beginner typists. By automatically checking for correct technique, the burden of checking each student is reduced, and directed interventions for bad habits can be easily created as students with these bad habits are easily identified.

This research has a direct impact on people that have hand or wrist injuries that are caused by poor typing habits. By correcting these poor habits, pain from these injuries will be reduced, and even be prevented from occurring in the first place. A specific example of this is by reducing ulnar deviation which affects the nerve that is indicative of CTS (Toosi et al., 2015).

Chapter 2

Review of Related Literature

2.1 Keyboard Typing

Keyboard typing is the process of using a keyboard to input characters in a system. In the context of this paper, keyboard typing will refer to the act of using a physical keyboard to input characters into a computer system.

2.1.1 Keyboard Layouts and Form Factors

One key characteristic of a keyboard is its physical attributes. Keyboards come in a lot of layouts and form factors. Keyboard layouts are the shapes, size, and positions of a key on a keyboard while the form factor of a keyboard refers to its shape and dimensions. The form factor also refers to the number of keys included in the keyboard (Parkkinen, 2018). By combining different layouts and form factors, different permutations of a keyboard can be created.

Different keyboard layouts and form factors also produce different effects for the user. This is due to how vastly different some keyboard layouts and form factors are from one another. Some layouts focus on ergonomics, while others focus on typing speed. Some form factors were designed for aesthetics, while others focus on comfort and health. As such, different layouts may affect typing performance, ergonomics, and long-term health effects (Ciobanu et al., 2016).

ANSI and ISO Layout

There are two common keyboard layouts around the world — International Organization for Standardization (ISO) and ANSI.

ANSI INCITS 154-1988 is the standard that first defined the ANSI layout. Figure 2.1 illustrates what the ANSI layout looks like. This layout is also used by countries other than America. Examples of countries that use this layout as its standard are the Philippines, China, and Korea (Apple, 2021). However, these countries also opt to modify the layout by adding extra layers to accommodate other character sets.

ISO/IEC 9995-1:2009 is the standard series that defines a framework that is used to create other layouts. Layouts created from this standard are colloquially called ISO Layouts. Countries around the world use this framework to create layouts that fit the characters in their language. Examples of countries that use this framework to create their layout are France, Greece, Canada, and Sweden (Apple, 2021).

Both of these layouts usually utilize the same key ordering. This ordering is commonly called QWERTY, based on the first five characters of the first row of this specific layout.

There are other layouts available, however, they are not as common as the two previously mentioned layouts. Examples of this include Japanese International Standards (JIS). Other esoteric layouts, like Tsangan or split-backspace, also exist. These layouts modify the ISO and ANSI standards by adding or removing certain keys to fit the character set of a language, or for additional keys. Other layouts are also the same as ANSI or ISO, however, these layouts change the arrangement of the alphabet within the keyboard.

Despite the ubiquity of these common layouts, studies have shown that these layouts are not ergonomic. The main issue with these layouts is the random configurations of the letters. The randomness of the layout necessitates memorization of the layout which reduces the ease of learning, reduces performance in typing by reducing speed, and increases typing errors (Ciobanu et al., 2016).

Keyboard Form Factors

There is only one common keyboard form factor used worldwide: the full-size keyboard. This keyboard contains all the keys specified in the keyboard layout. This includes the alphanumeric keys, the function keys, the navigation cluster, and the Numpad.

Other common keyboard form factors are based on the full-size keyboard. The name of these layouts, 60%, 75%, and 80% reference the remaining number of keys after cutting a portion off from the full-size keyboard. The 60% keyboards only contain the alphanumeric cluster while the 80% and 75% layouts retain the navigation cluster and the function keys (Parkkinen, 2018). The main draw for using keyboards with reduced sizes is for aesthetics, space constraints, and ergonomics.

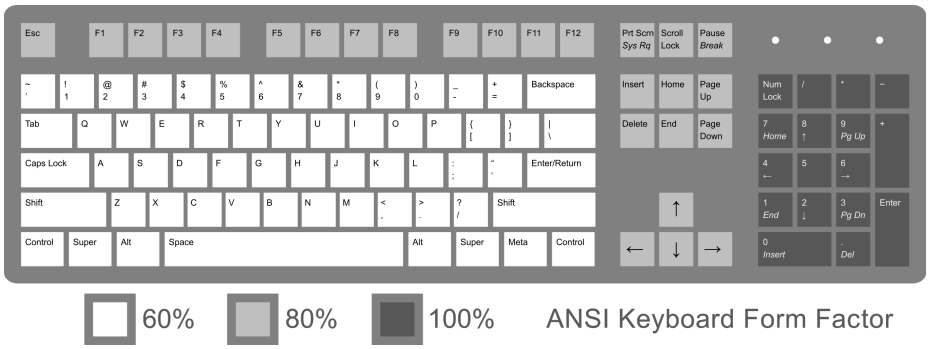

Figure 2.1: ANSI Keyboard layout with form factors. Reprinted from Rumudiez. (2013). Correctly labeled modifier keys for the ANSI Keyboard layout. Retrieved October 18, 2021, from https://commons.wikimedia.org/wiki/File:ANSI_Keyboard_Layout_Diagram_with_Form_Factor.svg

Ergonomic Keyboards Layouts and Form Factors

There have been other keyboard layouts and form factors created to mitigate common issues associated with QWERTY layouts. These include Colemak, Dvorak, and Alphabetical layouts. However, studies have shown that the layout itself does not matter as beginners do not necessarily see the keyboard as a structured set, but rather as a random collection of characters, even if it is alphabetized (Norman & Fisher, 1982),

A different form factor has a great effect on ergonomics. One such example of a form factor is an ergonomic keyboard developed by Microsoft called Microsoft Natural MultiMedia Keyboard. Ripat

et al. used this keyboard in determining that ergonomic keyboards can help in reducing symptoms of Work-related neck and upper limb disorders (WRNULD). Figure 2.2 shows the layout of the Microsoft Natural MultiMedia Keyboard.

Figure 2.2: Microsoft Natural MultiMedia Keyboard. Reprinted from DraugTheWhopper. (2014). MS Natural Multimedia Keyboard. Retrieved October 28, 2021, from https://commons.wikimedia.org/wiki/File:MS_Natural_Multimedia_Keyboard.png

There are other form factors other than the full-size keyboard and variations thereof that focus on ergonomics. One such example is a split keyboard layout where the keyboard is split in half, one for the left hand and one for the right. One such benefit, according to Ergodox EZ, is a more relaxed position due to typing at shoulder width.

2.1.2 Keyboard Typing Metrics

There are numerous metrics used to quantify keyboard typing performance. Two common metrics used in the majority of typing tests include Accuracy and Speed.

Standardized Keyboard Typing Assessments

To be able to measure these metrics, a keyboard typing assessment needs to be done. However, there are no standardized keyboard typing assessments (Donica et al., 2018). As such, teaching methods

and assessments, like Keyboarding without Tears, Monkeytype, and Keybr, may produce different metrics for the same typist due to their difference in conducting the assessment.

Speed

Speed, also called as entry rate by Arif and Stuerzlinger, measures the number of characters entered within a specific time frame. The most common metric that measures speed is WPM. WPM as defined by Arif and Stuerzlinger is:

$$WPM = \frac{|T| - 1}{S} \cdot 60 \cdot \frac{1}{5} \tag{2.1}$$

Where, $|T|$ is the length of the text, S is the time in seconds spent writing the text. This time starts directly after the first character has been pressed, and ends when the last letter has been entered. As such, 1 is subtracted from $|T|$, as the time spent to find and press the first character cannot be accurately determined. However, some typing assessments do not subtract 1 from $|T|$. 60 refers to the number of seconds in a minute and $\frac{1}{5}$ normalizes the metric for the average length of words.

Other metrics also measure speed, but they aren't as commonly used as WPM. These include Characters per Minute, Gestures per Second, Adjusted Words per Minute, and Keystrokes per Second

Accuracy

Accuracy measures the number of correctly pressed characters in an input string. Accuracy, as defined by Bartnik, is:

$$ACC = \frac{|C|}{|T|} \cdot 100\% \tag{2.2}$$

Where $|C|$ is the number of correct characters and $|T|$ is the length of the text.

The inverse of accuracy is error rate, where the number of incorrectly pressed characters is measured instead. Arif and Stuerzlinger describe 5 common error rate metrics: Error Rate, Minimum String Distance Error Rate, Keystroke per Character, Erroneous Keystroke Error Rate, and Total Error Rate.

Limitations of the Metrics

These metrics are all based on the inputted characters by the user. These metrics do not take into account other aspects of keyboard typing such as posture, hand and wrist positions, and finger placement. Consequently, these metrics do not give a full picture of the performance of the person typing, and they only provide a cursory view of how a person types.

2.1.3 Keyboard Typing Methodology

Keyboard typing can be accomplished in numerous ways. The main difference between the different methodologies is the number of fingers used when typing and how the typist navigates the keyboard to find the keys. The methodology ranges from Hunt and Peck to Touch Typing, with variations of the two in between.

Hunt and Peck uses one finger on one hand to press a key. This method is aided by using vision to locate the specific key to press (Hoot, 1986). On the other hand, Touch typing uses standard QWERTY mapping to type without using visual cues. (Dobson, 2009) This mapping involves assigning certain fingers to certain keys. Figure 2.3 is the standard QWERTY mapping used for an ANSI layout. Kinesthesis and proprioception are used in locating the keys (Logan et al., 2016).

Figure 2.3: Standard QWERTY mapping for ANSI. Reprinted from Logan, G., Ulrich, J., & Lindsey, D. (2016). Different (key)strokes for different folks: How standard and nonstandard typists balance Fitts' law and Hick's law. *Journal of Experimental Psychology: Human Perception and Performance*, *42*(12), 2084–2102. https://doi.org/10.1037/xhp0000272

2.1.4 Typing Speed Statistics

Median typing speed using a keyboard with QWERTY layout, based on test data from "keybr.com - Typing lessons" (2021), is $\approx$ 37.5 WPM. This median is taken from all the test results they have gathered from all of their users.

Bartnik (2022) released a dataset showing the speed of 12678 members of the Monkeytype community with the speed role. The dataset shows the fastest time that these members have achieved on 60-second tests. The median of the dataset lies in the 100–109 WPM range, with 52.74% of the community having top speeds slower than 100 WPM.

Arif and Stuerzlinger (2009) also performed a survey with 12 participants using multiple typing methods. They got an average WPM of 75.85 with a standard deviation of 15.61 when their participants used a physical QWERTY layout. This average WPM was also the highest among the other typing methods the researchers studied.

2.2 Keyboard Typing in Education

Today, students are expected to type essays, articles, and other submissions using word processors (Poole & Preciado, 2016). Testing is also commonly done using computerized assessments which require the need for keyboards (UMass Amherst, n.d.). As such, there is a need for students to be well versed in keyboard typing and for keyboard typing to be part of the curriculum.

Keyboard typing has been a part of this curriculum for a long time, with studies about effective methods to teach keyboard typing reaching as far back as 1986 (Hoot, 1986). Studies have continued to this day to continue to optimize and improve methods of teaching keyboard typing to students.

These studies start teaching kids at the kindergarten level and the studies try to optimize the teaching methods to improve the speed and accuracy of typing of the learners. By starting to teach touch typing to students early, these students will develop the potential for higher-level keyboard typing (Donica et al., 2018).

2.2.1 Expectations of Keyboard Proficiency

In the United States, keyboard typing is an expected learning outcome for third grade in the Common Core State Standards (Common Core State Standards Initiative (CCSS), 2010). At this grade level, only basic keyboard typing skills are required. By fourth grade, students are expected to have enough proficiency to type one page in one sitting. This is increased to two pages by fifth grade.

In the Philippine context, the Department of Education expects learners with a mental age of 4–6.9 years old to use correct posture and locate characters, learners with a mental age of 7–11.9 are introduced to home row finger placement, and learners with a mental age of 12 and above are expected to "use proper typing technique with efficiency and accuracy without looking at the keyboard" (Department of Education, 2020).

2.2.2 Current Teaching Methods

Current teaching methods involve replicating a given text. Learners then copy the text into a given text field that records the typed characters. Correct and incorrect characters are then identified, and suitable errors are presented. Afterward, metrics, such as WPM, and accuracy are given ("About TypeRacer," 2021; Bartnik, 2021).

Through this process, the learner goes through the three stages of Motor Learning Theory. The student undergoes the cognitive stage where they try to understand and create strategies to accomplish the given task. Then the associative stage follows where the strategies and skills learned from the previous stage are refined. At this stage, the learners are expected to rely less on visuals to locate the keys and more on kinesthesis. In the final stage, the autonomous stage, the learner does not rely on visuals at all and focuses on using kinesthetic feedback to find the keys. By this point, the learner has progressed from using Hunt and Peck, to becoming proficient in touch typing. (Donica et al., 2018)

Keyboarding without Tears

Keyboarding without Tears is a web-based application and curriculum that teaches students touch typing. However, one key differentiator of this curriculum is the usage of a row-based standard mapping, rather than a column-based standard mapping that is common in other teaching guides. Figure 2.4 shows the standard mapping used in this curriculum.

This curriculum is self-directed and learners can learn at their own pace. At its core, the curriculum is designed to be 36-week long with 5–10 minutes of lessons per day. The lessons in the curriculum follow the three stages of Motor Learning Theory ("Keyboarding Without Tears — K-5," 2020).

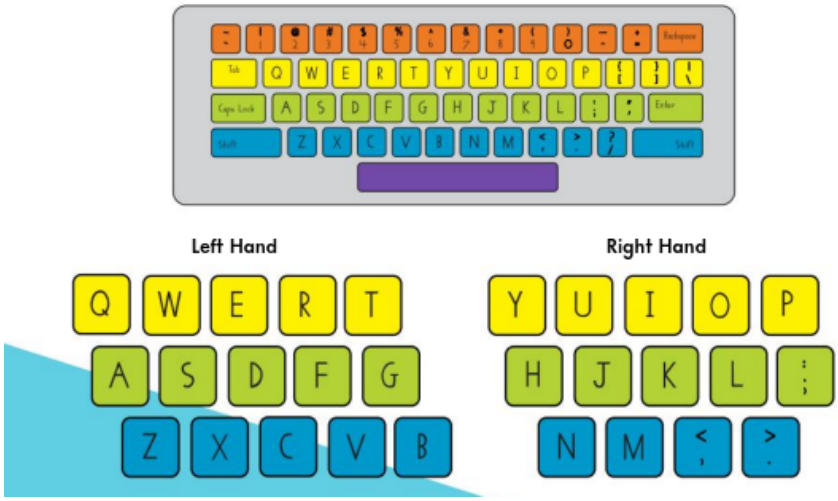

Figure 2.4: Row based standard mapping. Reprinted from Keyboarding Without Tears — K-5. (2020). Retrieved October 26, 2021, from https://issuu.com/handwritingwithouttears/docs/kwtbrochure2020/1

Monkeytype, Typeracer

These two keyboard typing tests are similar. They follow a common experience where users type a predetermined phrase, quote, or random words, and metrics are given after the test. Afterward, the learners may try the test again, or choose another set of words to type. These typing tests do not have a structured curriculum for learning how to touch type. It is left to the learner to practice and learn on their own ("About TypeRacer," 2021; Bartnik, 2021).

Keybr

Keybr is similar to Monkeytype and Typerace, in that they also have the users type a predetermined phrase, quote, or random words. However, this application has more guidance compared to the two. Keybr uses statistics to create typing lessons that are appropriate to the current typing proficiency of the learner. The words selected are random at first, and the skill level of the learner is determined by the performance of the user with these words and characters. The information gathered is then used to generate new words for the next iteration. As an example, if a learner has difficulty typing the letter q, the next iterations will have a lot of words that contain the letter q.

Statistics from their website show that this learning method is successful, with some learners improving their typing speed by 20–40 WPM ("keybr.com - Typing lessons," 2021).

2.3 Keyboard Typing in Health

There have been a lot of studies that show the effect of keyboard typing, and its associated movements (or lack thereof), affects the human body. These studies have shown that keyboard typing affects our neck, shoulder, upper limb, wrist, arms, and fingers (Baker, Cham, Hale, et al., 2007; Szeto et al., 2005)

2.3.1 Health Issues arising from Keyboard Typing

WRNULD are a common issue that is associated with an elongated length of time maintaining a static posture. When using the computer, the posture commonly adapted by users has the neck and shoulder regions in a static hold for a long time. This results in forward neck flexion and increased muscle tension (Szeto et al., 2005).

In addition, it has been shown that 22% of computer users sustain musculoskeletal disorders of the upper extremity. This includes the neck, shoulder, hands, and wrists. (Gerr et al., 2002)

Carpal tunnel syndrome is also a common issue in the general population. This is caused by the chronic compression of the median nerve. There is a common belief that typing is one main cause for the disorder (Operations, 2021). There are no definite conclusions if this myth is true, however, a study by Toosi et al. found that typing causes ulnar deviation, especially if done without proper form. This ulnar deviation contributes to the swelling of the median nerve during and after typing. However, the authors noted that it is unclear if this swelling leads to long-term nerve injury.

2.3.2 Finger and Wrist Kinematics

The way people move their hands, wrists, and fingers differs between each person. This can be attributed to the different typing styles each person has. One key difference between people is the angle of the fifth digit.

However, there are some common movements and positions regardless of typing style: flexion, or the curving of the fingers, across the fingers, is decreasing across the hand, with the 2nd digit having the least flexion. This may be due to the instinct to reduce pronation of the hand, which in turn increases the distance of the 2nd digit to the keyboard. In addition, some people isolate or extend one of their thumbs, usually the one not used for pressing a key. This is also true for some people that do not use their fifth digit during typing (Baker, Cham, Cidboy, et al., 2007).

The movement and angle of the wrists also depend on the typing style of the typists. Some people do not reposition their hands, while others do. This difference comes from the way these people reach for certain far-away keys. Some stretch their fingers to reach far-away keys, while others move their entire hand to reach these keys.

For those that reach their keys by stretching their fingers, there is an increased probability that the wrists and fingers adapt to non-neutral postures. These include wrist extension, ulnar deviation, and pronation, which may cause musculoskeletal disorders of the upper extremity (Marklin et al. (1999) as cited in Baker, Cham, Cidboy, et al. (2007))

2.4 Finger and Hand Tracking

Finger and Hand tracking is a method of tracking fingers and hands in 3D space using motion capture systems or computer vision. This technique allows computers to perform actions and analyzes the motions and positions of these body parts.

2.4.1 Types of Tracking

Hardware Aided Solutions

Motion Capture Systems allow for capturing detailed skeletal motion in humans. These systems usually capture full-body motion, focusing on large parts of the human body, such as the torso, limbs, and head.

However, motion capture systems have difficulty in tracking more articulated body parts — with

the fingers being one of them. The industry standard for capturing finger movements is through the use of an optical marker-based motion capture system. This is due to its ability to capture natural motion accurately.

This method uses cameras to triangulate the 3D location of markers attached to the limbs of a person. For finger tracking, 13–20 markers are placed on the fingers, and cameras are brought closer to track the small movements of the finger (Wheatland et al., 2015).

But this method is cost-prohibitive, and cannot handle occlusions well. Alexanderson et al. present a method for an optical marker-based motion capture system that can predictably recover from self-occlusion and has a better performance compared to previously used algorithms, however, the issue of cost and self-occlusion persists.

Bend-sensor gloves are also an option for finger tracking. These gloves have sensors within them that track joint angles in the hand and fingers. One key differentiator of this solution compared to the others is the removal of self-occlusion in the data. As such, this is commonly used in sign language, and gesture recognition due to its accuracy.

However, these gloves need a lot of time to calibrate as cross-coupling of the sensors proves a problem. Cross-coupling is prevalent because the movement of one finger also moves other parts of the hand. These movements may cause a sensor aimed to track a specific movement of a different part of the hand to inadvertently detect a movement when there should be none (Wheatland et al., 2015).

Computer Vision

At its core, Computer Vision aims to perform tasks that the human visual system can do (Huang, 1996). This includes object classification, tracking, gesture recognition, and face recognition. At the present, most computer vision systems utilize deep learning algorithms, and convolutional networks to gather information from an image, or a set of images. One such example of a convolutional network used in computer vision is Inception by Szegedy et al. which proposes a convolutional neural network architecture for object classification and detection.

2.4.2 Available CV Solutions for Tracking

OpenCV

OpenCV is an open-source library that provides ≈ 2500 optimized algorithms for computer vision and machine learning. This library is widely used by companies, researchers, and open source communities that utilize computer vision and machine learning in their projects. Examples of companies that use OpenCV include Google, Sony, and Honda.

The library has C++, Python, Java, and Matlab interfaces. The library also supports Windows, Linux, Android, and macOS, allowing for great developer experience, and wide deployment capabilities (Bradski, 2000).

MediaPipe

MediaPipe is an open-source computer vision framework that allows developers to create a perception pipeline. This perception pipeline is a directed graph of calculators. Data passes through the graph as packets and a group of packets constitutes a data stream. As the data passes through the pipeline, the calculators, produce the desired output.

This framework allows for performant object detection, hand and finger tracking, and human pose detection. The framework also allows for combining multiple features, by adding them to the graph as calculators. MediaPipe has C++, Python, JS, and Coral interfaces. It also supports Android and iOS devices (Lugaresi et al., 2019).

Examples of projects that utilized MediaPipe and its solutions include a real-time hand gesture recognition system by Sung et al. (2021) which utilized MediaPipe Hands. Another example is by Wu and Senda (2021) which utilized MediaPipe Hands to track movements during pen spinning competitions. Halder and Tayade (2021) developed a real-time sign language recognition program using MediaPipe Hands.

MATLAB

MATLAB is a programming platform for the analysis and designing of systems. MATLAB is commonly used by engineers and scientists for computational mathematics (MathWorks, 2021b).

A toolbox offered by MATLAB is the Computer Vision Toolbox which contains algorithms, and functions for use in the development of computer vision, 3D vision, and video processing systems. By using the available algorithms in the toolbox, such as YOLOv2, and ACF, hand detection and gesture recognition is made possible in the platform (MathWorks, 2021a).

2.4.3 Applications

There have been multiple applications and products that utilize hand and finger tracking as their main component.

Dorfmuller-Ulhaas and Schmalstieg (2001) present a use case for finger tracking in augmented environments. In the paper, interaction in a virtual environment through the use of gestures. The tracking system uses an optical marker-based motion capture system where the user wears a glove with retroreflective markers.

Hsu et al. (2014) used a Kinect, a 3D sensing device by Microsoft that uses depth data, to track fingers to play virtual instruments. Virtual Pianos and Guitars were created and played with reliable and stable tracking.

Yousaf and Habib (2014) created a virtual keyboard that operates using finger tracking. The tracking uses the movement of the finger joints as the basis for selecting which key to press. The tracking first detects where the hands are. The result of the detection is then piped to a different algorithm for finger joint localization. These are then used to generate finger joint trajectories using kernel tracking. A Dynamic Bayesian Network then uses feature vectors from these trajectories to classify, detect, and recognize keystrokes.

2.5 Summary of the Research Gap

While there are a lot of applications and curricula aimed at teaching touch typing, there is no automated system available that detects if a person uses the correct finger to press a key.

By having this system, educators can accurately determine if and when a student is having a hard time typing and if these students will need an intervention to correct mistakes.

This is also important because certain movements and hand positions will cause nerve and muscular disorders that will impact the user. By correcting these problematic movements and hand positions, these disorders can be prevented.

Chapter 3

Methodology

This section provides an overview of the development and testing of a real-time finger-key identification module. First, the experimental setup used for data collection will be presented. Following that, the algorithm used to implement real-time finger-key identification will be discussed. The process of training and testing of the developed algorithm comes next. Afterwards, the development and design of the proof of concept trainer will be described. Finally, this section introduces two metrics that were developed to quantify correct finger placement during typing tests.

3.1 Setup

The experimental setup and configuration were composed of three elements: the camera, the keyboard, and the environment. This setup was used to collect data points to measure the algorithm's ability to perform finger-key identification in a controlled environment. Figure 3.1 is an image of the experimental setup.

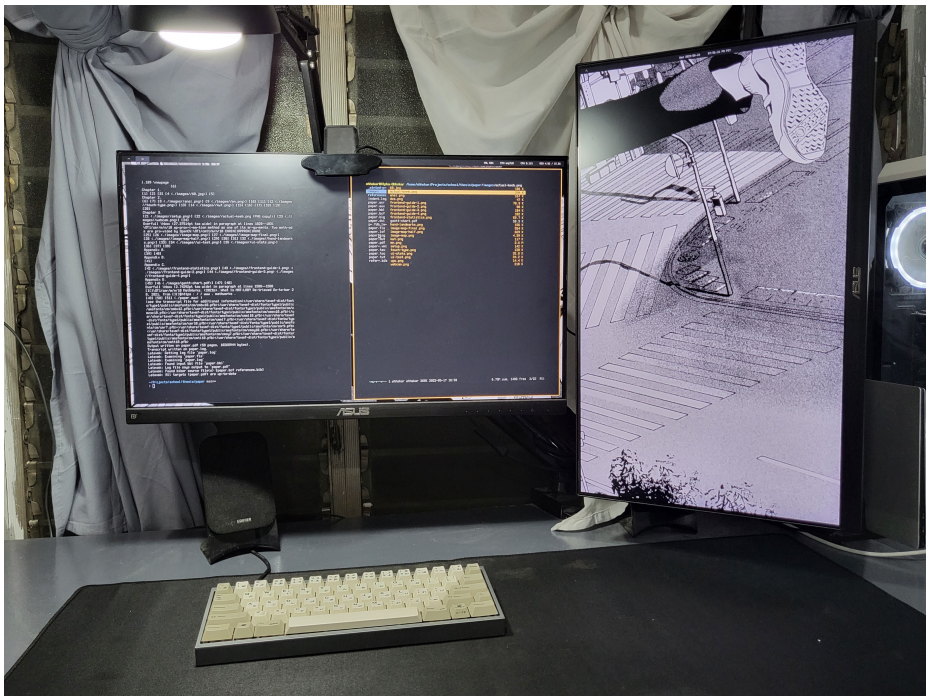

Figure 3.1: The experimental setup

3.1.1 Camera

The setup used a single monocular camera positioned in a top-down view. The camera captures the entirety of the keyboard and the movement of the ten fingers. To do so, it was mounted on top of the monitor with the camera pointed down towards the table. Figure 3.2 illustrates how the camera was mounted over the monitor and Figure 3.3 is a picture taken with the camera at this position.

Figure 3.2: The camera angled downwards to capture the keyboard

Figure 3.3: Image captured by the camera in one of the training iterations

The specific camera used was a Logitech C920. It is a 3 mega pixel webcam that is capable of capturing color video in 1080p/30fps and 720p/30fps with a diagonal field of view of 78°. For the setup, the camera captured the video in 480p/30fps. This camera has a universal mounting clip that allows the camera to be correctly positioned within the experimental setup ("Logitech C920 PRO HD Webcam, 1080p Video with Stereo Audio," n.d.).

3.1.2 Keyboard

The keyboard used was a 60% keyboard as shown in Figure 3.3. This limited the necessary mapping for the algorithm to the alphanumeric portion of the keyboard. This keyboard choice also reduced the area that the camera captured, as this keyboard type is considerably smaller compared to a full-size keyboard. The keyboard also had its keycaps and case in a light color that contrasted the dark surface it was placed on. It also had a dark USB-C cable to blend with the dark surface. These color coordination steps improved initial keyboard detection.

In addition, the keyboard layout was a modified ANSI layout. The majority of the keys remained the same, however some keys were changed: the pipe key was replaced by the backspace key, the backspace key was replaced by the pipe key and a delete key, and the bottom row has a longer spacebar. Overall, these are minor changes that does not affect the alphanumeric keys that are predominantly used in typing.

3.1.3 Computer

The computer used to run the algorithm is a desktop computer. The specifications of this computer is shown in Table 3.1.

Table 3.1: Computer Specifications

Component	Specification
CPU	AMD Ryzen 5 3600
GPU	AMD Radeon RX 5600 XT
RAM	G.Skill Trident Z Neo RGB 16GB 3200mhz
Storage	Samsung SSD 850 EVO
OS	Arch Linux

3.1.4 Environment

The setup was lit with a lamp besides the camera. This light source evenly lit the keyboard and the fingers used for typing. The light source used was a common LED bulb rated at 9 watts with 700 lumens. This light is white with a color temperature of 6500k.

In addition, the surface where the keyboard was placed was solid black without any variation of color. This also improved initial keyboard detection.

3.2 Algorithm

3.2.1 Computer Vision based Keyboard Detection, and Key Mapping

A computer vision algorithm was created as a starting point for mapping the keys of the keyboard within a video. A rough flowchart of the algorithm is shown in Figure 3.4.

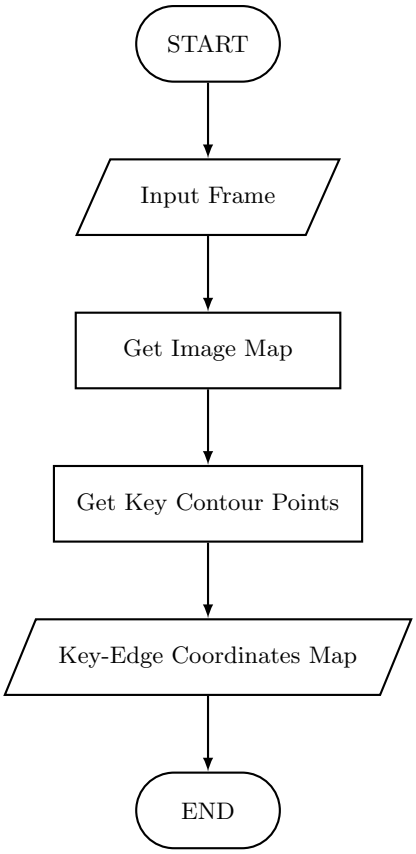

Figure 3.4: Flowchart of Keyboard Detection and Mapping Algorithm

Get Image Map

The first portion of the algorithm creates an image map that is overlaid over the detected edges of the keyboard. The flowchart for this function is shown in Figure 3.5.

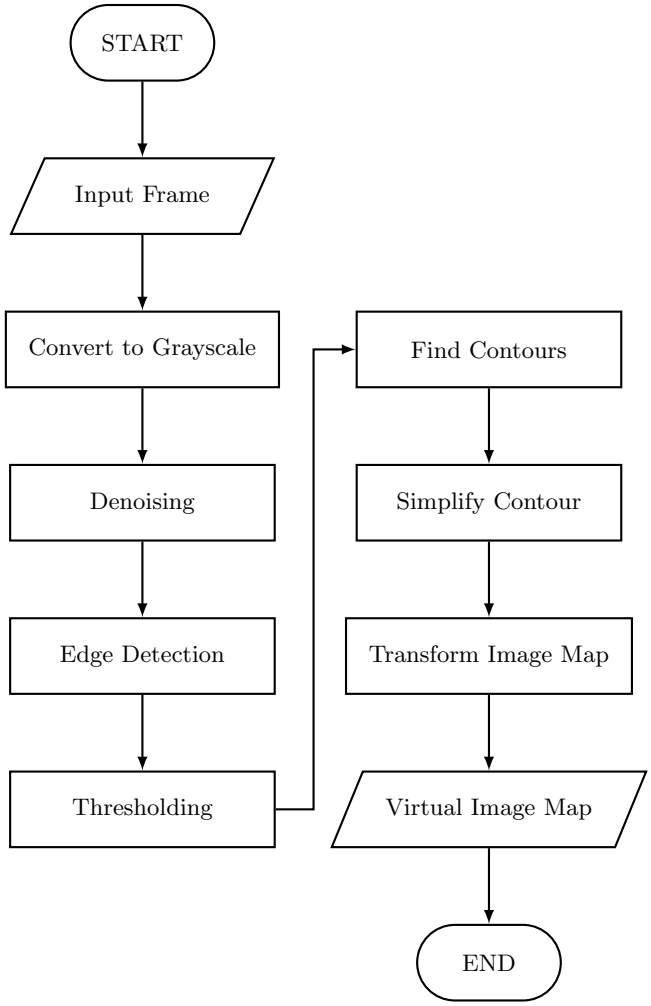

Figure 3.5: Flowchart of Get Image Map

Convert to Grayscale The input frame from the camera was converted to a 256 level grayscale image using `cvtColor` of OpenCV ("OpenCV: Color Space Conversions," n.d.). This step was performed because future steps of the algorithm did not require color values to work. In addition, this step optimized the algorithm as the number of dimensions analyzed was reduced. Figure 3.6 is the output of this step.

Figure 3.6: Camera capture converted to grayscale

Denoising The algorithm denoised the grayscale image using a bilateral filter as implemented by OpenCV ("OpenCV: Image Filtering," n.d.). This filter takes the range of the image into account, rather than just the domain. This resulted in an image that is smoothed while preserving its edges (Fisher, n.d.). Figure 3.7 is the output of this step.

Figure 3.7: Smoothed image with intact edges

Edge Detection The algorithm used a Sobel filter for edge detection. This filter uses a 3×3 kernel that is convolved twice — once horizontally, and another vertically — to produce a grayscale image of the outlines within the frame. The kernels used by the Sobel filter (Sobel, 2014) is shown in Figure 3.8 and the output of this step is shown in Figure 3.9.

$$\begin{bmatrix} +1 & 0 & -1 \\ +2 & 0 & -2 \\ +1 & 0 & -1 \end{bmatrix} \begin{bmatrix} +1 & +2 & +1 \\ 0 & 0 & 0 \\ -1 & -2 & -1 \end{bmatrix}$$

Figure 3.8: Sobel Operator Kernels. Reproduced from Sobel, I. (2014). An Isotropic 3x3 Image Gradient Operator. *Presentation at Stanford A.I. Project 1968*

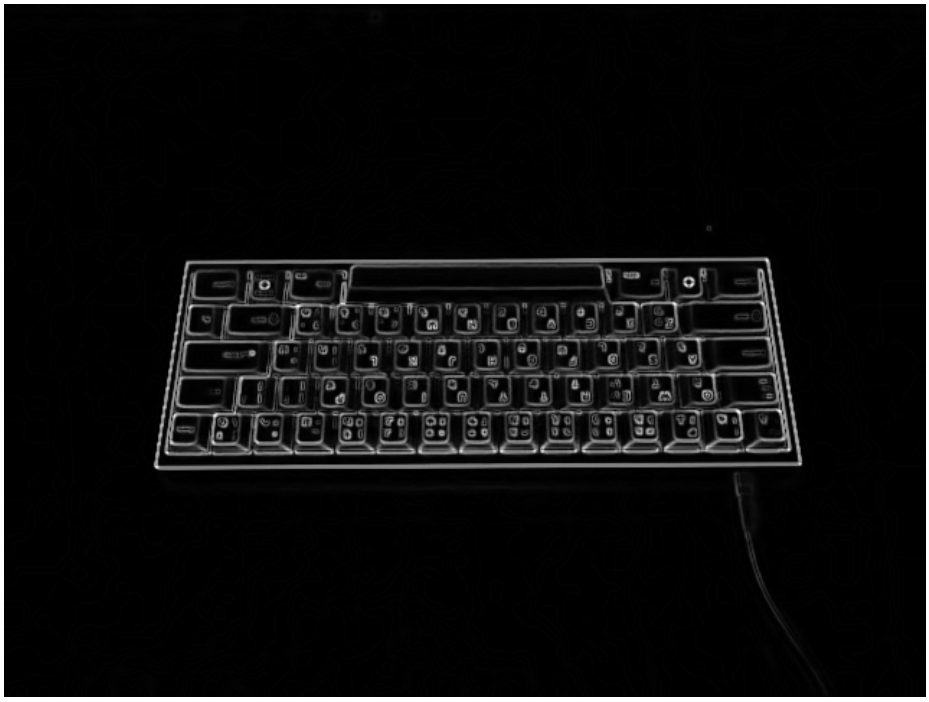

Figure 3.9: Output of the Sobel filter

Thresholding The output of the Sobel filter is a grayscale image of 256 values, with each gray pixel indicating edges within the image. There is a need to reduce the range of these values to improve the ability of the algorithm to find the contours of these edges. To do so, the algorithm utilized Otsu's algorithm to perform automated thresholding. Otsu's algorithm determines a single threshold that is most optimal for the image (Otsu, 1979). This outputs a black-and-white image, with only two values. Figure 3.10 is the resulting output of this step.

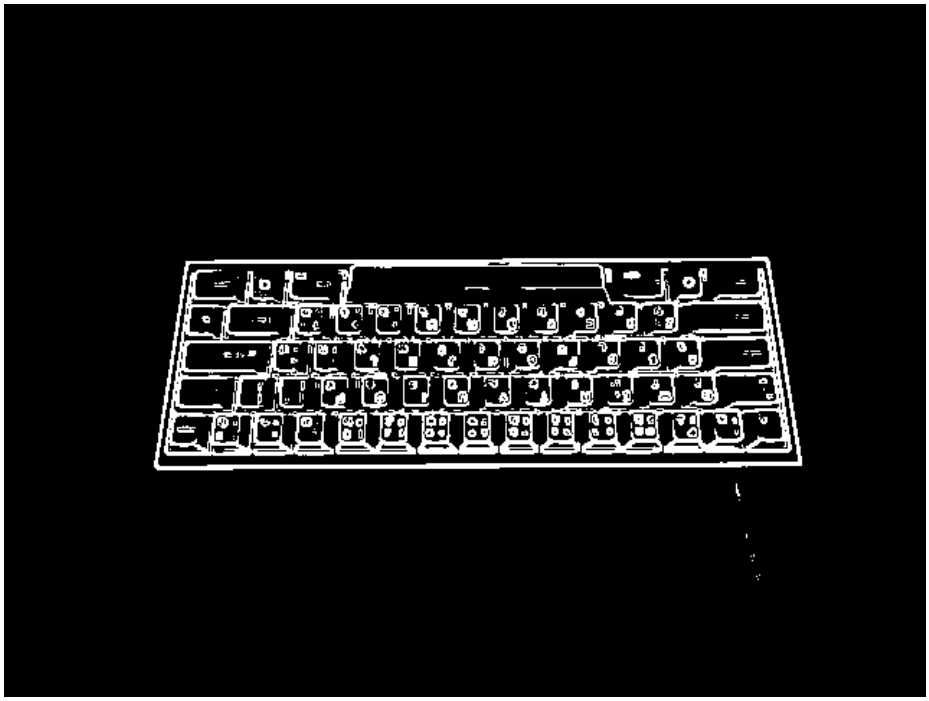

Figure 3.10: Threshed image of the edges

Find Contours Contours are curves joining all continuous points that have the same color or intensity ("OpenCV: Contours : Getting Started," n.d.). The OpenCV function `findContours`, with the `CHAIN_APPROX_SIMPLE` contour approximation method, was used to find the contours of the outlines of the object found using the previous step. This approximation method removed redundant points and returned the least amount of points that describe the shape. This OpenCV function implements the algorithm of Suzuki and Abe (1985) in their paper "Topological structural analysis of digitized binary images by border following." Figure 3.11 shows the contours found in the threshed image.

Figure 3.11: All the contours found in the image

Simplify Contour However, the points returned by the function can contain more than the four extreme points at the edges of the keyboard. In addition, more than one contour may be found within the image. As such, the algorithm sorted the contours by area, and selected the largest one.

After sorting, the algorithm performed the Douglas-Peucker algorithm for Line Simplification (Saalfeld, 1999). This reduced the number of points in the largest contour to the minimum amount. In ideal cases, the number of points would be four, with each point corresponding to the edges of the keyboard. However, there were times when other objects would be within the frame, or they intersected with the keyboard. This would result in a contour that would be defined by more than four points — which caused the entire algorithm to fail.

The contour points that described the contour were then sorted clockwise. This was a necessity since the algorithm of Suzuki and Abe (1985) does not guarantee that the largest contour's points were returned in a clockwise arrangement. There is a need to have consistent ordering of these points since the transformation that will be performed in the next step pairs the contour points to a hard-coded array that indicates the edges of the image map. This hard-coded array was sorted clockwise. As such, if the contour points were not sorted clockwise, there will be no guarantee that

the pairing would result in a transformation that creates a transformed image map that is oriented correctly, since the pairing may not pair the correct points.

Figure 3.12 shows the four contour points found at the edges of the keyboard within the image.

Figure 3.12: Simplified contour

Transform Image Map The virtual keyboard map is a rectangular image that contains individual Region of Interest (ROI) for each key in a 60% ANSI keyboard. Each key has a corresponding color assigned to it and this color fills the region where this key is located at. Figure 3.13 is the initial image map and Appendix A is a table that lays out the mapping of the color code in BGR format and its associated character in the image map.

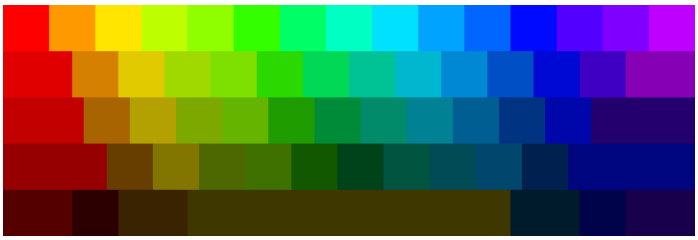

Figure 3.13: Initial Image Map

The virtual map was stretched over the keyboard using OpenCV's `warpPerspective` function. The function requires a perspective transform that was calculated using `getPerspectiveTransform`. This function takes in two arrays with four points each. The input points are the edges of the virtual map, ordered clockwise. The output points are the four points of the contour, ordered clockwise ("OpenCV: Geometric Image Transformations," n.d.). The resulting transform was then used by `warpPerspective` to apply the transform to the virtual map. Figure 3.14 is the image obtained after warping the image map.

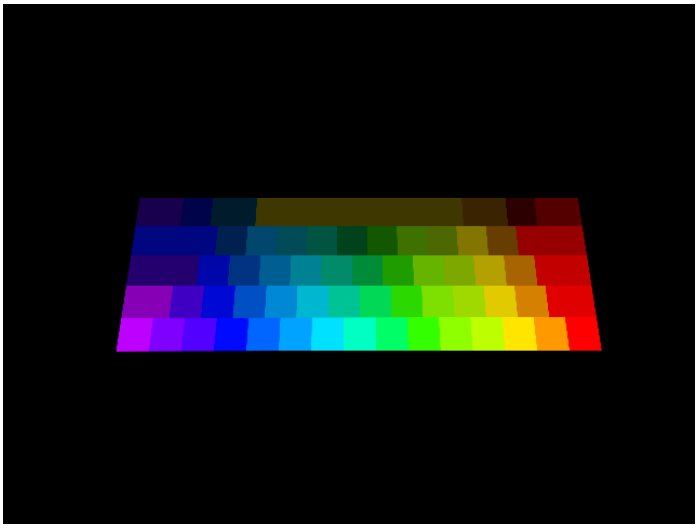

Figure 3.14: Transformed image map

Get Key Contour Points

The second portion of the algorithm pre-computes the contour points of each key in the keyboard based on the generated virtual map and the Key-Color Values map. The flowchart of this function is shown in Figure 3.15

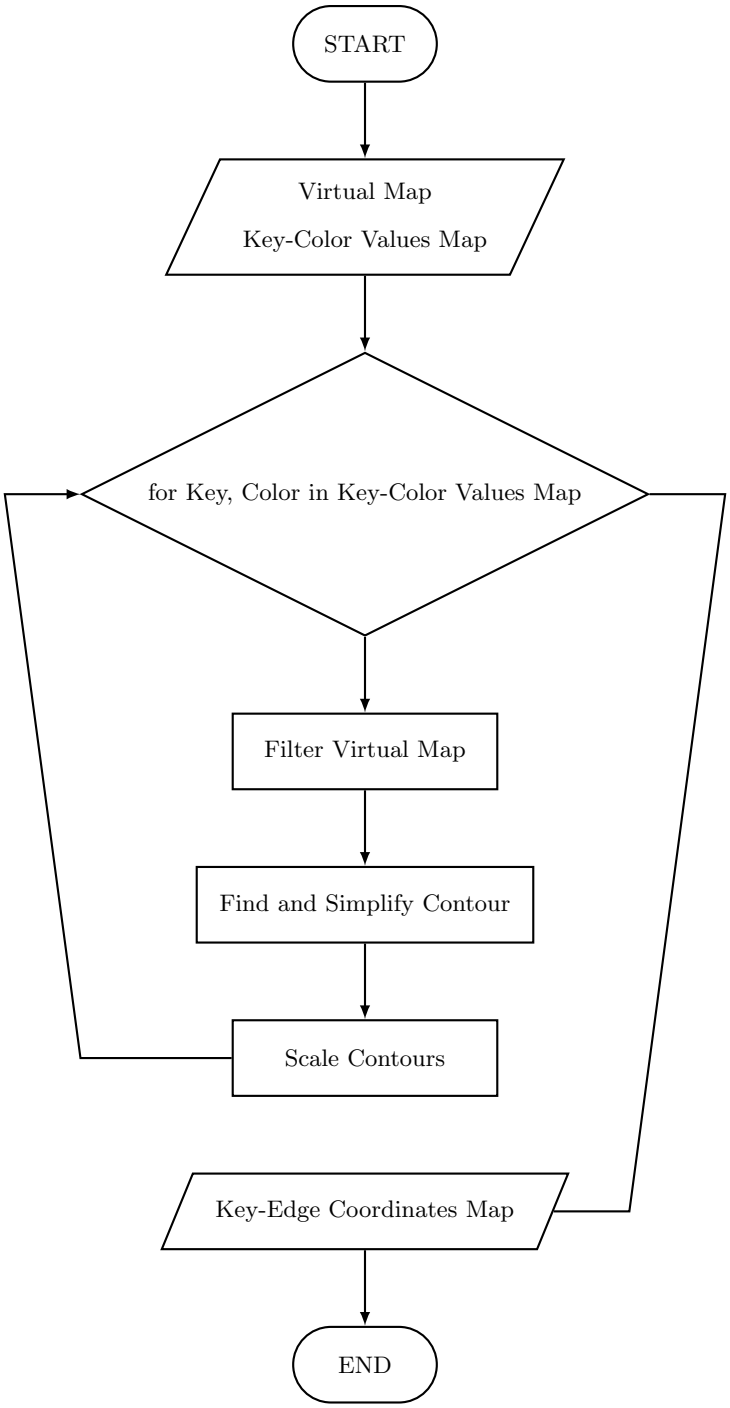

Figure 3.15: Flowchart of Get Key Contour Points

Filter Virtual Map The color that corresponds to each key in the virtual map is stored in the Key-Color Value Map. This color was used to create a mask for the virtual map for a specific key. This mask was obtained by using this snippet of code `(virtualMap == key).all(axis=2)`. This

mask was then used to black out the rest of the virtual map, leaving only the ROI of the key in the image.

This specific method was used as the other method that was trialed, `np.where(virtualMap != key)`, did not consider all 3 channels when comparing each pixel — i.e. a key assigned with the color value of `[100, 0, 0]` will not be blacked out if the color value of the key to be isolated is `[100, 243, 0]` as the blue channel of the pixel, `100` is equal in both. This would result in other keys remaining in the virtual map, even if only one key corresponds to that color. Figure 3.16 shows the image where the Left Control key was isolated.

Figure 3.16: Filtered key

Find and Simplify Contours The same method in finding and simplifying the contour of the keyboard was used to find and simplify the contour of the ROI of the key. Figure 3.17 illustrates the four edges of the isolated key.

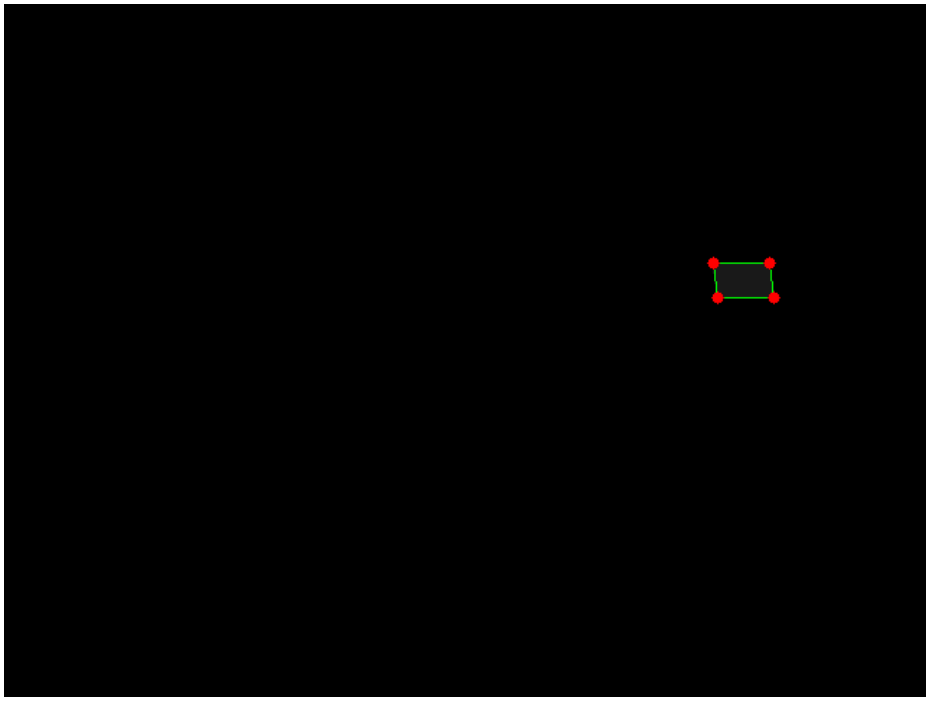

Figure 3.17: Contour points of the ROI

Scale Contours During testing using training data, a lot of the failures in finger-key identification were due to the tight fit of the contour to the key. The contour on its own did not give enough buffer for the placement of the finger. This buffer was needed as, in some instances, the finger used to press the key was not exactly on top of the key, but rather to its side. In addition, it can also be observed that the finger tracking does not annotate the very edge of the fingertip, but rather, it labels somewhere in the middle of the fingernail.

The algorithm accounts for this situation by adding a buffer. This was achieved by scaling the contour points by seven pixels on each side. Figure 3.18 shows the increased buffer in relation to the key. This value was obtained after testing other possible values. A buffer of five pixels did not have a lot of effect in reducing the number of failures. A buffer of ten pixels did reduce the number of failures, but it also greatly increased the algorithm's uncertainty in determining the finger — uncertainty is defined as detecting two or more fingers within one ROI. Seven was a good middle ground in decreasing failures, without greatly increasing uncertainty.

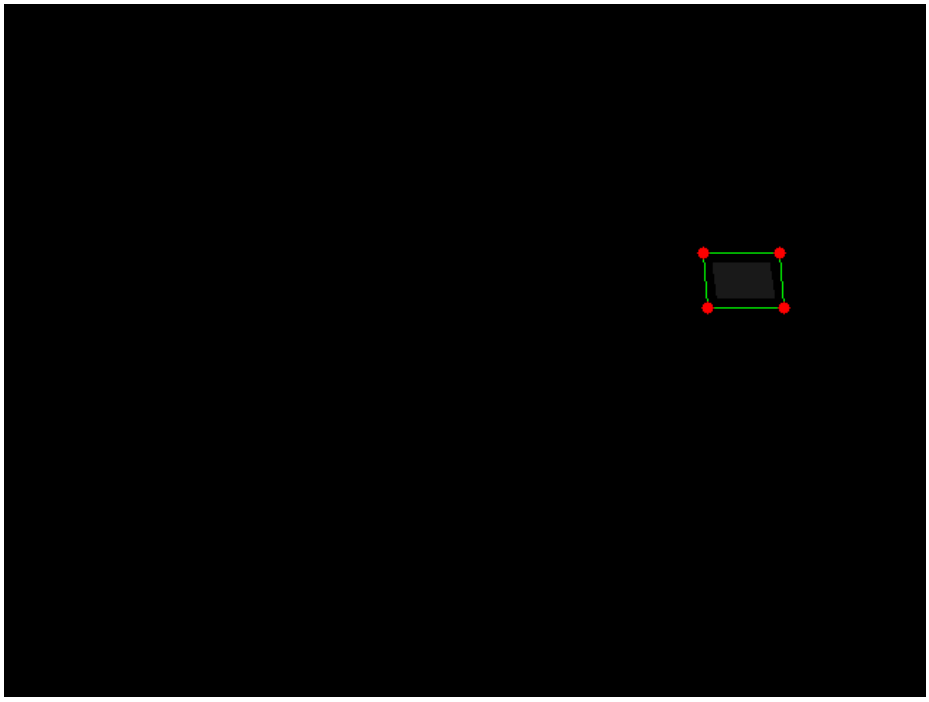

Figure 3.18: Scaled contour points of the ROI with the buffer of seven pixels

Key-Edge Coordinates Map After all the keys have passed through the loop, a Key-Edge Coordinates Map was generated. Each key now has four points that serve as the coordinates of the edge of its ROI.

The coordinate system that the contour points are based on had its origin at the top left, starting at 0, 0. Going to the right increased the value of the x-axis, and going to the bottom increased the value of the y-axis. This results in a coordinate system that only has positive values with each value corresponding to a pixel.

3.2.2 Computer Vision based Finger Detection, and Tracking

MediaPipe Hands was used as the finger detection and tracking solution. This algorithm is composed of two ML models working in conjunction to be able to detect the different parts of the hands and track them accurately.

Palm Detection Model

The first model, the Palm Detection Model detects the initial hand locations using a single shot detector model based on the paper by Liu et al. (2016). This model achieves an average precision of 95.7% in palm detection (Lugaresi et al., n.d.).

MediaPipe Hands detects the palms first, instead of whole hands with one model because hands lack high contrast patterns. This reduces the model's ability to detect hands with accuracy. In addition, detecting a palm is simpler compared to detecting hands with articulated fingers since estimating a bounding box around a rigid object, i.e. a palm is much simpler. Furthermore, a palm can be modeled using only square anchors reducing the number of anchors by a factor of 3–5 (Lugaresi et al., n.d.).

Hand Landmark Model

After the palms have been detected and an appropriate anchor has been established, the Hand Landmark Model pinpoints 21 3D hand-knuckle coordinates inside the detected hand. This is done using direct coordinate prediction.

This model was trained using 30,000 manually annotated, real-world images with 21 3D hand-knuckle coordinates. Using this information, the model can also accurately add landmarks to partially visible hands and hands with self-occlusion. This is also made possible by the model's consistent internal hand pose representation (Lugaresi et al., n.d.).

3.2.3 Integration for finger-key identification and mapping

The two previously chosen algorithms were combined to accomplish finger-key identification and mapping.

The integration of the algorithm was a two-step process. The first step was to get the Key-Edge Coordinates Map shown in Section 3.2.1.

The second step runs whenever a key press has been detected. This step used the Key-Edge

Coordinates Map in conjunction with the finger tracking algorithm selected in Section 3.2.2. The flowchart of the algorithm is shown in Figure 3.19

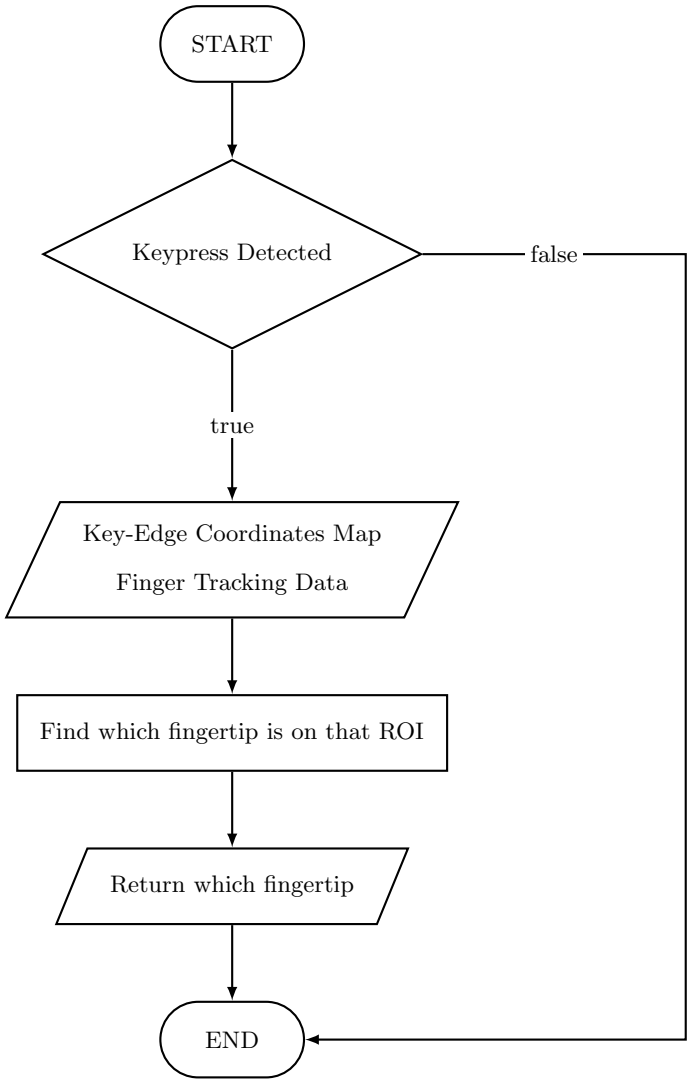

Figure 3.19: Flowchart of the overall flow

Find which fingertip is on that ROI

The Finger Tracking Data contained the pixel positions of each landmark of the hand. For this step, the algorithm finds the landmark which is positioned within the single ROI obtained from the previous step. This was done using a series of checks.

Each landmark's coordinates were compared to the coordinates of the edges of the ROI. A landmark was determined as positioned within the ROI if all the following conditions are true:

1. On the X-axis, the landmark's coordinates are greater than one or both of the two coordinates found on the left side of the ROI
2. On the X-axis, the landmark's coordinates are less than one or both of the two coordinates found on the right side of the ROI
3. On the Y-axis, the landmark's coordinates are greater than one or both of the two coordinates found on the top side of the ROI
4. On the Y-axis, the landmark's coordinates are less than one or both of the two coordinates found of the bottom side of the ROI

These conditions maximized the total area of the ROI, and it is not strict about exact accuracy. In essence, these conditions create a perfectly rectangular box that contained the quadrilateral formed by the four points from the coordinates. Figure 3.20 is an example of a frame with a successful finger-key identification using the conditions previously mentioned.

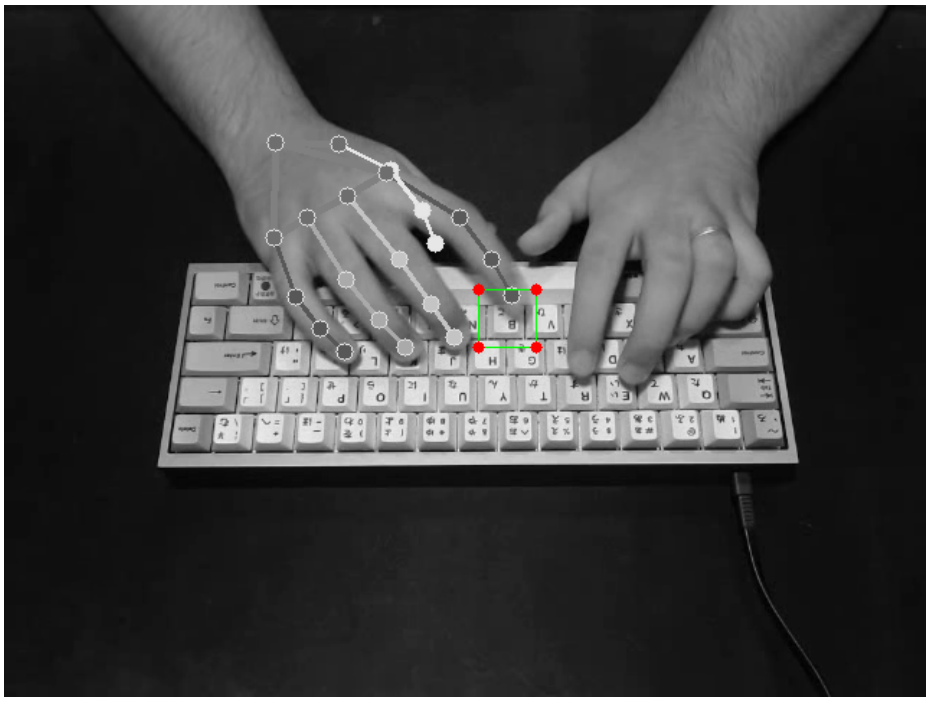

Figure 3.20: Fingertip within an ROI

Return which fingertip

The landmark was then used to determine which specific finger corresponds to the key press. Figure 3.21 shows each possible landmark that may be returned from the previous step. This step returned the name of the landmark, up until the first underscore. As an example, if the landmark found is `MIDDLE_FINGER_TIP`, this step will return `MIDDLE` denoting that the middle finger is the finger that corresponds with the key press. In addition, the specific hand will also be returned as one of two strings, `LEFT` and `RIGHT`, since this information is also bundled together with the landmarks. The two strings were then concatenated with an underscore. An example return value is `RIGHT_RING`.

As such, the expected output of the module is the hand and the finger used to press the key. This allows for a more flexible utilization of the data as it carries greater context, compared to just returning if the finger used was correct or not.

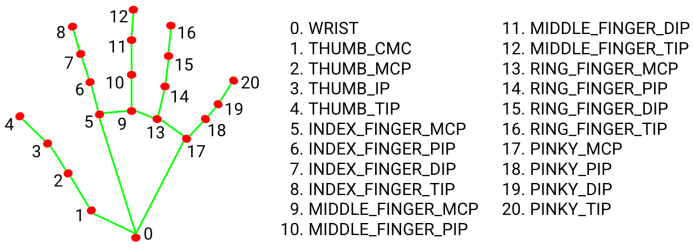

Figure 3.21: Hand landmarks that may be returned by the algorithm. Reproduced from Lugaresi, C., Tang, J., Nash, H., McClanahan, C., Uboweja, E., Hays, M., Zhang, F., Chang, C.-L., Yong, M., Lee, J., Chang, W.-T., Hua, W., Georg, M., & Grundmann, M. (n.d.). Hands. Retrieved January 13, 2022, from https://google.github.io/mediapipe/solutions/hands.html

.

3.2.4 Implementation

The previously discussed algorithms were implemented using Python. The Keyboard Detection and Mapping Algorithm in Section 3.2.1 was implemented as a separate module in Python using OpenCV. The Finger Detection and Tracking Solution in Section 3.2.2 was implemented using the prebuilt Python package offered by the MediaPipe team. Finally, the integration of the two was done as another separate module in Python.

3.3 Training and Testing

3.3.1 Typing Test Sequences

Typing test sequences are strings that were used in testing the user in their ability to type. The test sequences that were used came from text found in the public domain obtained from Project Gutenberg and the Internet Archive. Sentences were isolated from these texts and used as test sequences if they fit the criteria.

The criteria for choosing test sequences were as follows: (1) $\approx$ 80% of the characters on the keyboard is present in a test sequence. (2) The number of words in a test sequence does not exceed 25. (3) Numbers and punctuations should be present in at least $\approx$ 30% of the total test sequences.

There was a total of 10 test sequences that were gathered. An example test sequence is "What of it, if some old hunks of a sea-captain orders me to get a broom and sweep down the decks?" from Moby Dick by Melville (2001). The 9 other test sequences can be found in Appendix Chapter B.

3.3.2 Data Gathering

Video Capture

There were 3 sets of 10 videos that were captured by the researcher, for a total of 30 videos. Each set corresponds to three predetermined speeds of typing: slow (15wpm), average (35wpm), and fast (80wpm). These speeds were based on test data from "keybr.com - Typing lessons" (2021). The researcher typed the 10 typing test sequences at these predetermined speeds. Best effort was made to stick to the predetermined speeds. During typing, errors were not consciously taken into account, and errors happened naturally as part of the typing process — with more errors happening more frequently as the typing speed increased.

A Python script was created to facilitate this process. The script captured a video of the researcher as the researcher was typing the test sequences. Whenever the researcher pressed a key, the corresponding frame count was captured, and the key pressed was recorded in conjunction. This

was stored in the format `FRAME_NO:KEY_PRESSED`, and each keypress was then stored as a line in a file.

One caveat of the camera used was its autofocus capabilities. This meant that there was a set amount of time during the start of the recording where the camera captured blurry images of the keyboard. This necessitates around three seconds for the autofocus to complete and focus on the keyboard. There was one video capture where the whole test sequence was scrapped as the researcher started typing even if the camera was not focused.

Keypress Labeling

The researcher then manually performed finger-key identification for all key presses present in the video. This was also done through a Python script. The script parsed the file associated with a video. The frame number found at each line was then shown, and the associated data with the frame was superimposed over it. Figure 3.22 is an example of a frame with these data overlaid over the captured image. The researcher then pressed keys that corresponded with the finger used to press the key. This was then again stored in the format `FRAME_NO:KEY_PRESSED:FINGER_USED`, and each keypress was then stored as a line in a file.

Figure 3.22: Screen showing the labeling process

Test-Training Split

The annotated data was then divided into training and test data at a ratio of 60:40.

Data Inventory

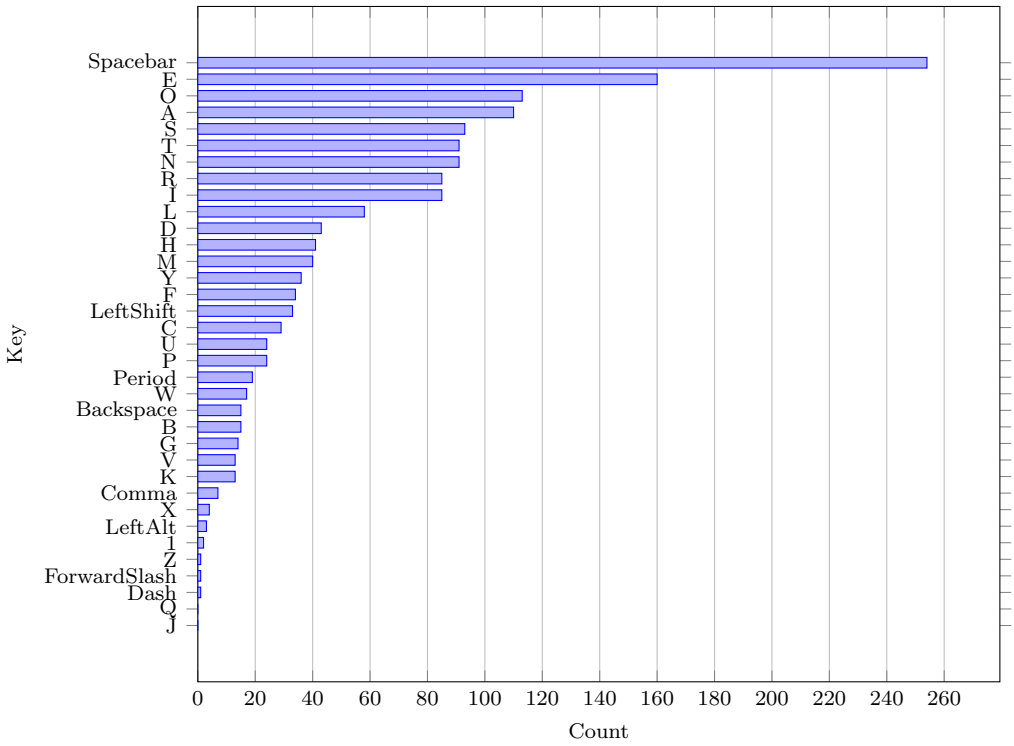

Figure 3.23: Training Dataset Inventory

Individual counts of the characters in the training iteration data set is shown in Figure 3.23. The letters were not represented equally in the data set. Of note, J and Q were not in the dataset.

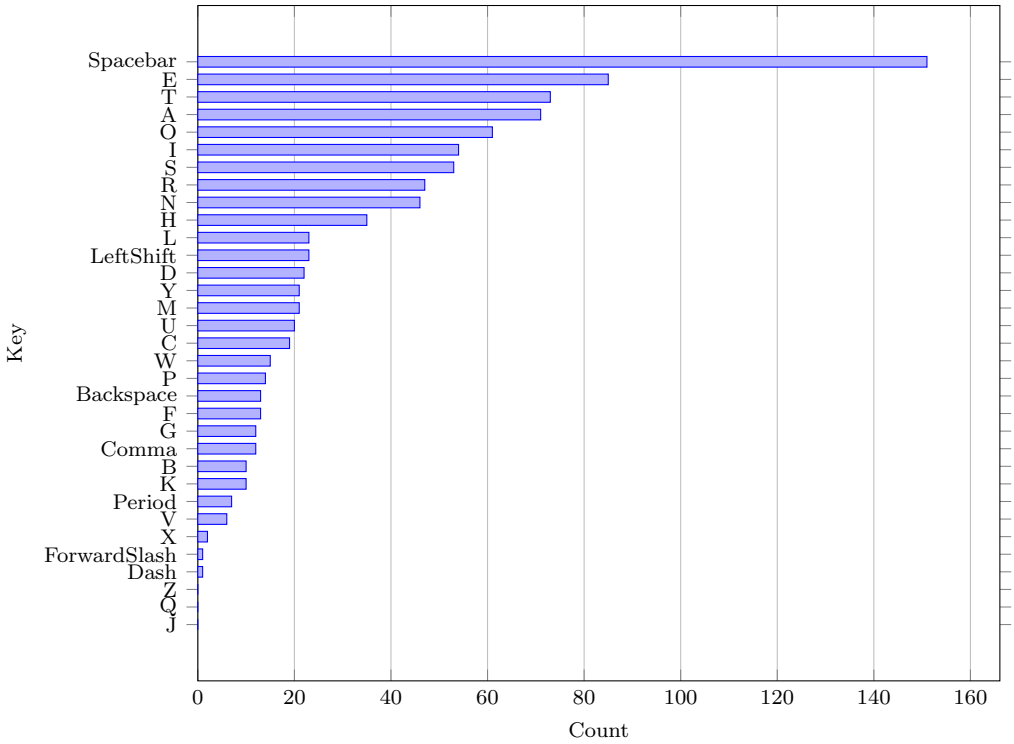

Figure 3.24: Test Dataset Inventory

The letters were also not represented equally in the test dataset as shown in Figure 3.24. Three characters in the alphabet were not represented in the dataset: J, Q, and Z. The inequality of representation in both of these datasets can be attributed to the source materials of the typing test sequences — novels and texts. While there were criteria to select which text was sourced, there was no conscious decision to equally represent all characters in the data set.

3.3.3 Training

A script was created to test the accuracy of the module. This script opened each video and the associated labeled file. There were three frames taken for each video to perform step one of the module: frames ten, fifteen, and twenty. The first frame that returned a Key-Edge Coordinates Map after going through step one of the module was used. The rest of the frames were not passed through the module and were discarded.

The script then parsed the labeled file and opened the frame for each keypress. The second

algorithm of the module was then run, using the data needed for the algorithm: the key pressed. The result of the module was then compared with the manual labeling of the keypress. The resulting data from the test was then stored in a `.csv` file with the following content:

Table 3.2: CSV File Contents

Column Name	Definition
`file_name`	Name of the file
`frame`	Frame number
`key`	Key pressed
`finger`	Manual labeling of the finger used to press the key
`is_correct`	If the module was correct
`fingertips_detected`	The fingertips detected by the module
`keyboard_detection_time`	Time spent in creating the Key-Edge Coordinates Map
`finger_classification_time`	Time spent in classifying which finger pressed the key

Adjustments were then made to the algorithm after each training pass to improve its performance. Some runs had improvements in their statistics without doing any adjustments. These were runs that showed errors in the manual labeling and were corrected afterward.

3.3.4 Analysis

The resulting `.csv` file was imported into Google Sheets and key statistics were obtained based on the data. Appendix C shows the screenshots where this was performed. The statistics obtained can be found in Table 3.3. These key statistics informed what to adjust in the algorithm and its overall performance.

Table 3.3: Acquired statistics

Identifications	
Successes	Number of successful finger-key identifications
Failures	Number of failed finger-key identifications
Success Percentage	Percentage of successful finger-key identifications
Failure Percentage	Percentage of failed finger-key identifications
Failure Types	
Mismatched Identification	Module output did not match manual labeling
No Identification	Module did not detect fingertips in ROI
Uncertain Successes	
Total	Total uncertain successes, defined as detecting two or more fingers within one ROI
Spacebar	All uncertain successes that were on the spacebar
Spacebar Percentage	Percentage of spacebar uncertain successes over all uncertain successes
Spacebar Percentage (Total)	Percentage of spacebar uncertain successes over total keypresses
Non-spacebar	All other uncertain successes
Non-spacebar Percentage	Percentage of non-spacebar uncertain successes over all uncertain successes
Non-spacebar Percentage (Total)	Percentage of non-spacebar uncertain successes over total keypresses
Average Running Time	
Keyboard Detection Time	Average keyboard detection time of all videos
Finger Identification Time	Average finger identification time of all key presses

3.3.5 Testing

The same script was run through the test data. The same format of output was gathered, and the same key statistics were recorded.

3.4 Trainer

A trainer was developed as a proof of concept of a real-world implementation of the finger-key identification module.

3.4.1 Design

The design was heavily based on Monkeytype by Bartnik (2021). Additional components were added to enable real-time finger-key identification. There are three main screens:

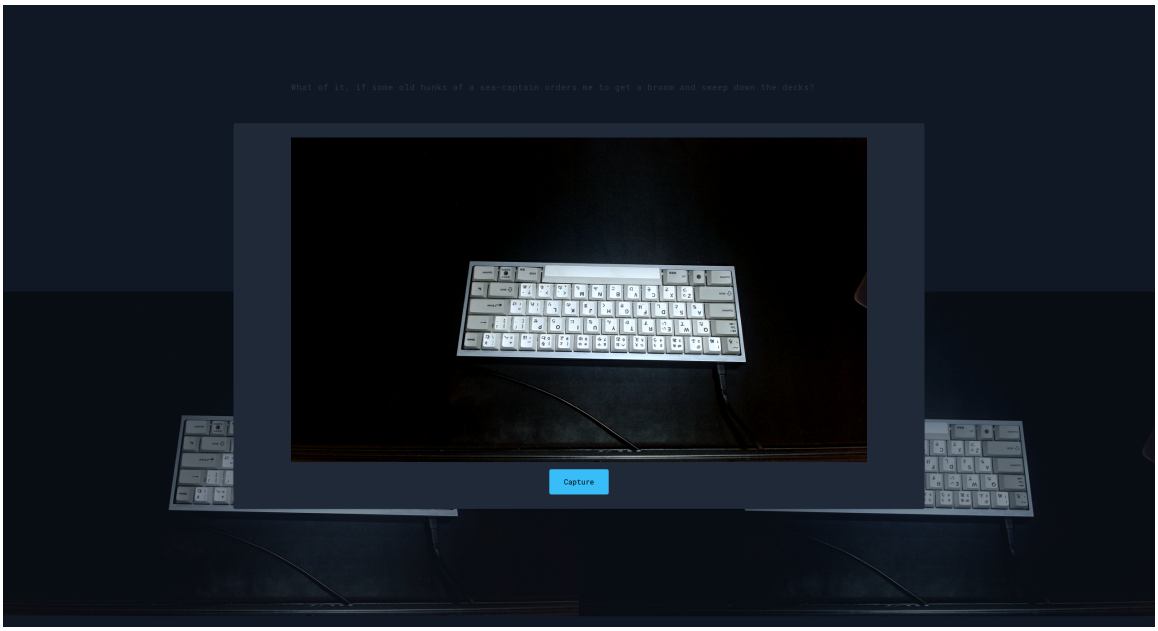

Figure 3.25: Frontend Screen for obtaining Key-Edge Coordinates Map

Figure 3.25 shows the first screen the user sees. This page captured the keyboard and passed it to the backend to obtain the Key-Edge Coordinates Map.

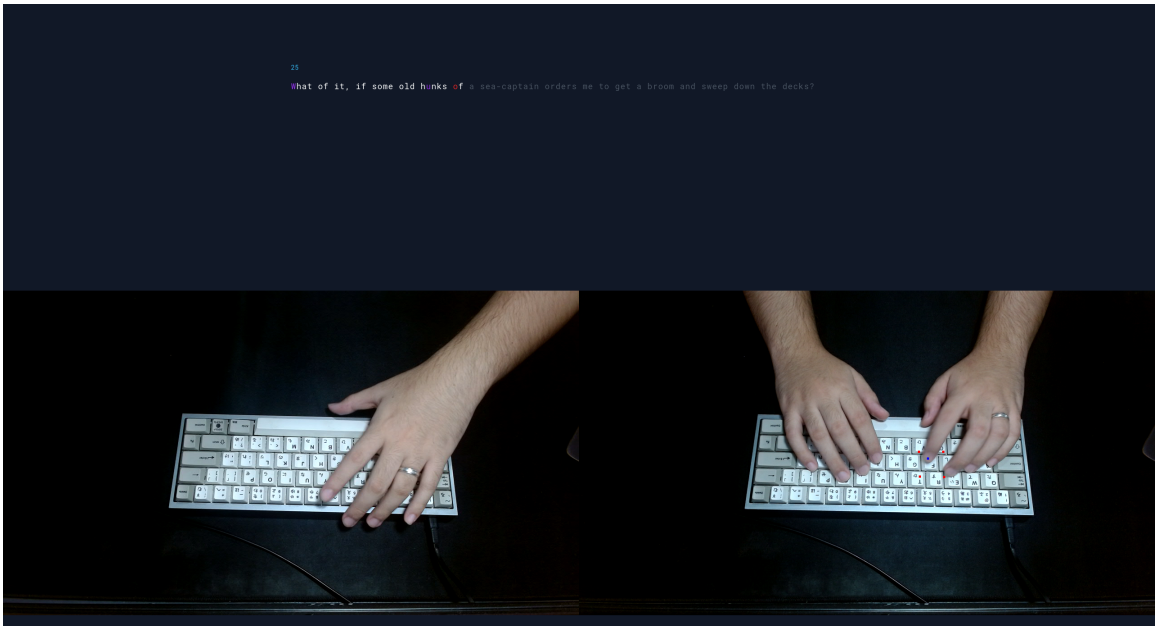

Figure 3.26: Testing page of the trainer

Figure 3.26 is the screen where the user performs the typing test. On this screen, the typing test sequence was placed above. If a letter was typed correctly with the correct finger, the character was colored white. If the wrong character was typed, the character was colored red. If the correct character was typed, but the finger used was incorrect, the character was colored purple.

At the bottom, the video captured by the webcam was shown on the left. Right beside it, important coordinates of the finger-key identification module are overlaid over the specific frame that was used as the input.

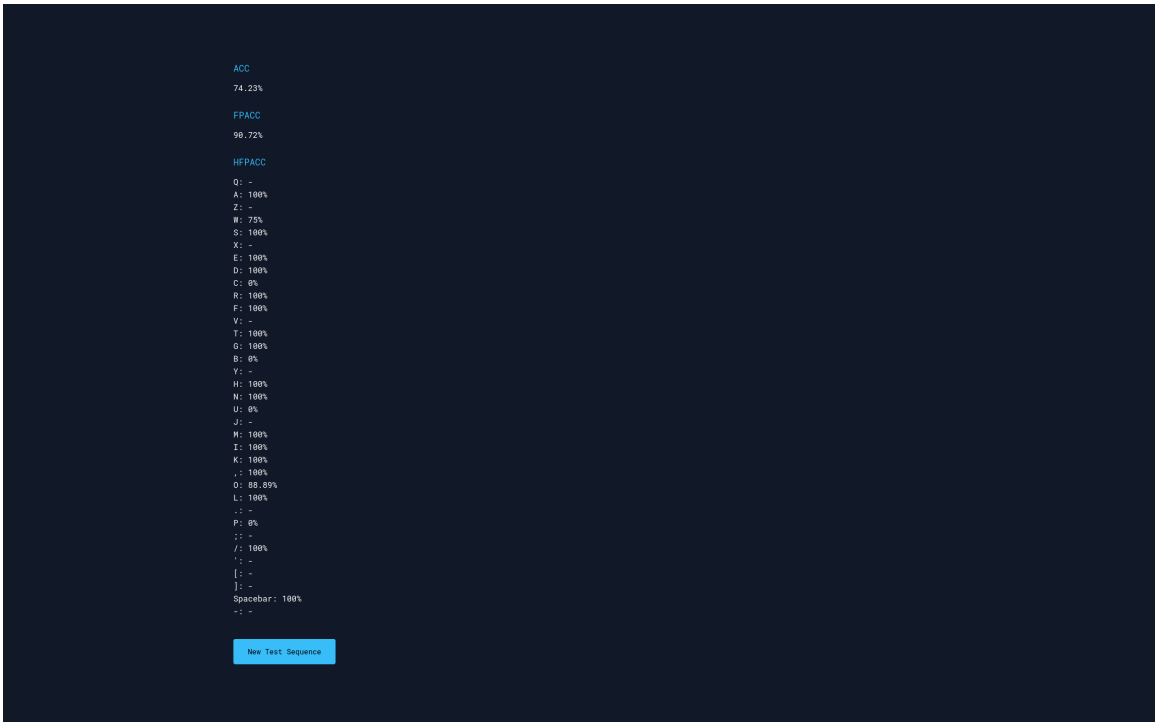

Figure 3.27: Page presenting the metrics obtained from the trainer

The metrics gathered from the test sequences are shown on a page as illustrated in Figure 3.27. This page presents metrics that will be discussed in Section 3.5. Of note, the metrics shown on this page that use multiple test sequences as an input uses tests that were obtained only during the time the page was opened. This proof of concept does not store the data of a user's previous test sequences that were performed from a different session.

Implementation

The frontend was developed in Svelte, and the backend was developed with Flask. The frontend handled capturing the video, presenting the layout, and capturing input events. Finger Tracking was done on the frontend through the use of MediaPipe Hand's JavaScript library. The frontend also handled checking what fingertip was inside the ROI of the key that was entered. The backend handled the generation of the Key-Edge Coordinates Map using the image passed from the frontend.

Two of the key steps in the module: finger tracking and integration were offloaded in the frontend as the wall of latency that exists between the frontend and the backend would cause performance

issues. While this issue also exists in obtaining the Key-Edge Coordinates Map, this wouldn't affect real-time finger-key identification since this is a preprocessing step and is not ran during the time the user performs the typing test.

3.5 Metrics

There were two total metrics obtained pertaining to finger and key mapping. The first was per test sequence, and the second was per key.

3.5.1 Per Test Sequence

The metric which calculates per test sequence is Finger Placement Accuracy (FP ACC). This metric computes the percentage of accurate keys pressed with the correct finger over the length of the typing test sequence. Inputting the wrong character, even if pressed with the correct finger, reduces FP ACC since FP ACC measures *accurate key presses*, and incorrect characters are considered inaccurate key presses.

The equation for calculating FP ACC is as follows:

$$FPACC = \frac{|F|}{|T|} \cdot 100\% \tag{3.1}$$

Where $|F|$ refers to the number of accurate keys pressed with the correct finger and $|T|$ refers to the length of the text.

3.5.2 Per Key

This metric, Historical Finger Placement Accuracy (HFP ACC), computes the accuracy of the user in pressing a certain key with the correct finger over all test sequences. The same criteria in determining accurate key presses. This allows the user to easily verify which keys need attention and training if there is a high frequency of error.

The equation for calculating a key's HFP ACC is as follows:

$$HFPACC_{char} = \frac{|F_{char}|}{|C_{char}|} \cdot 100\% \tag{3.2}$$

Where $|F_{char}|$ refers to the number of accurate keys pressed with the correct finger for a certain character, identified as $char$. $|C_{char}|$ refers to the number of times the character has appeared in all test sequences for the user.

Chapter 4

Results and Discussion

4.1 Accuracy

Accuracy, in the context of the finger-key identification module, calculates the percentage of successful finger-key identifications that the module has performed. In this case, success is defined as having the expected finger, based on the manual labeling, equal to the return value of the module. Accuracy is calculated as:

$$ACC = \frac{|S|}{|T|} \tag{4.1}$$

Where $|S|$ is the number of successful finger-key identifications, and $|T|$ is the total number of keypresses for all typing test sequences. This is also referred to as the success percentage.

4.1.1 Training Results

There were a total of seven training iterations. These training iterations served as a way to improve the performance of the module by adjusting its parameters.

Identifications

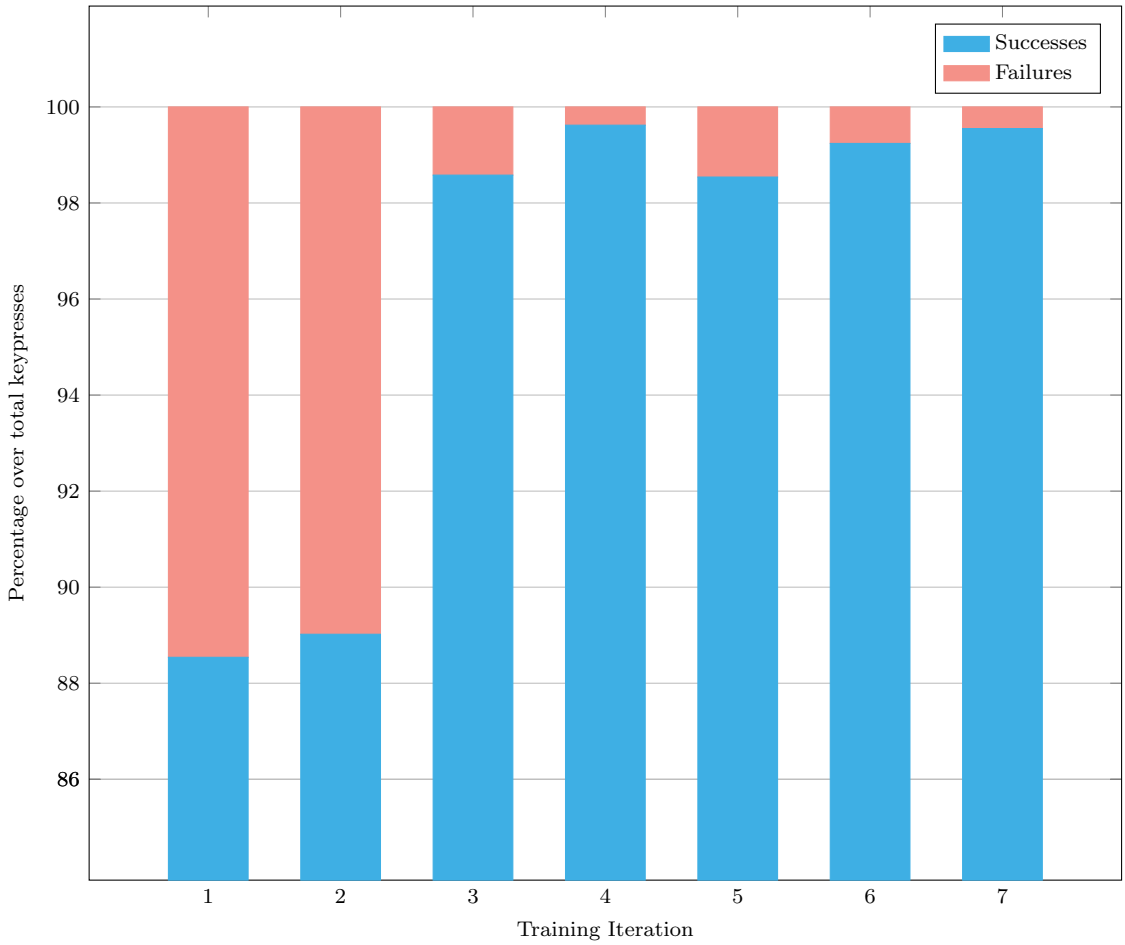

Figure 4.1: Identification results of the training iterations

Over the seven training iterations, there was an increase in success percentage as shown in Figure 4.1. Consequently, there was also a decrease in failure percentage. There was a total of 1475 total keypresses for iterations one to three, and 1571 total keypresses for iterations four to seven.

The increase in total keypresses starting from iteration four was due to adding multiple tries to the training routine in obtaining the Key-Edge Coordinates Map. Iterations one through three only tried frame 10 as the source frame for the module while iterations four through seven tried frames 10, 15, and 20.

There was a need to try different frames since the camera was not consistent in its ability to focus on the keyboard for each video. In some videos video, the camera was not focused on the keyboard in frame 10, but it was able to focus on frame 15. As a result, the total number of available keypresses to test increased.

The 0.48% jump between iterations one and two can be attributed to correcting erroneous finger-key identifications that were obtained from manual labeling. The 9.56% jump in success percentage between iterations two and three was due to adding buffers around the ROI by scaling the contours by 10 pixels on each side. Iteration four's increase was due to fixing the image map. Certain keys had incorrect color values assigned in the Key-Color Values Map, and some keys were of incorrect shape. Iterations five to seven were performed to test different values and shapes for scaling the ROI.

Uncertain Successes

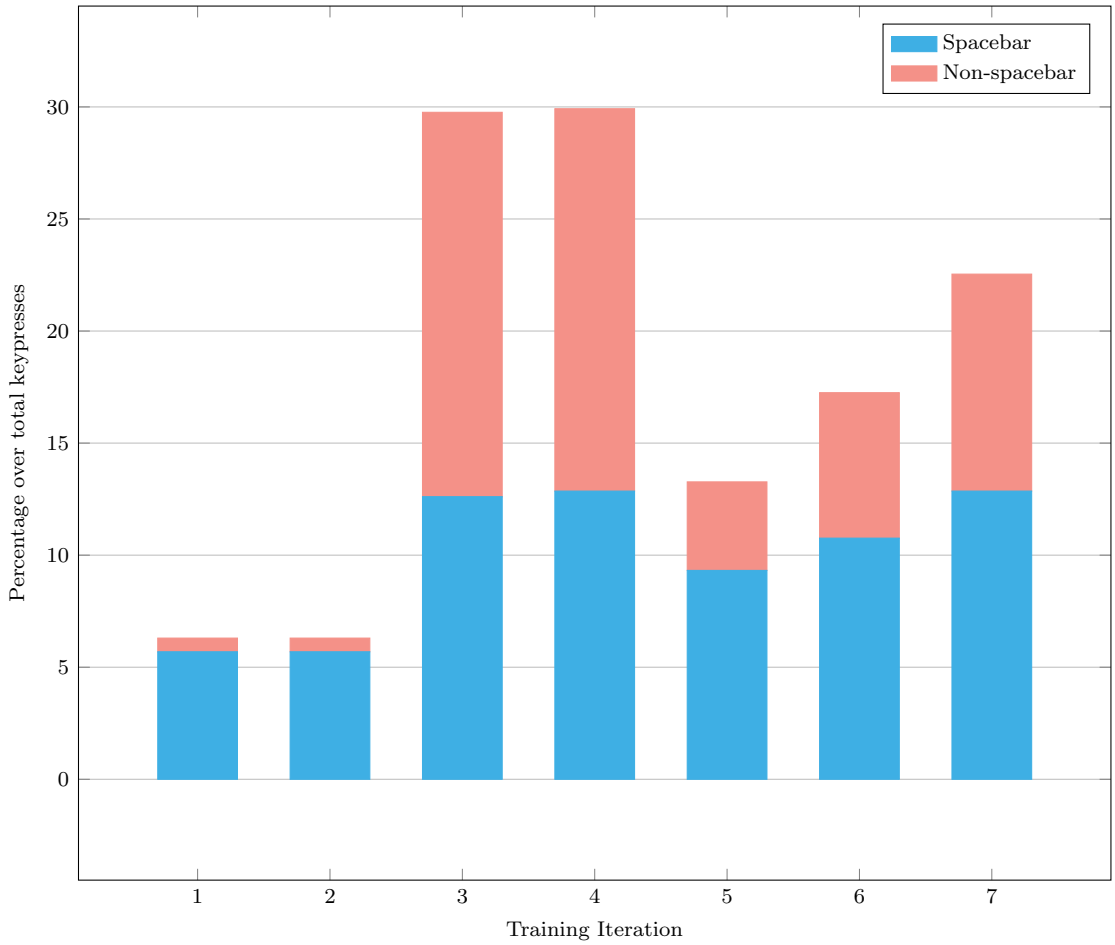

Figure 4.2: Uncertain Successes of the training iterations

Uncertain Successes are instances where the finger-key identification module was able to detect two or more fingertips within the ROI of the key. As such, the module is uncertain which of the multiple fingertips pressed the key. However, it is still classified as a success since the expected finger from the manual labeling exists within the array of fingertips returned by the module. Figure 4.2 shows the trend of this metric throughout the different training iterations.

Spacebar In a 60% keyboard, the spacebar is the longest key on the keyboard. In addition, this key is right below the non-dominant hand's thumb default resting position when the hand's posture

follows the proper touch typing posture. As such, it was to be expected that a majority of the uncertain successes were because of the spacebar. However, this was not the case for iterations three and four. This was because the buffer for the ROI was too big and this caused the module to detect more than one fingertip within that ROI.

Non-spacebar There were cases where the module had uncertain successes that were not over the spacebar. In almost practically all cases, these were over the alphanumeric keys. These uncertain successes stem from the increased buffer of the ROI. This type of uncertain success carries more weight compared to spacebar uncertain successes since the keys where these uncertain successes come from are the smallest keys on the keyboard. This means that the chances that a person has two or more fingers over the keys are rare, compared to the spacebar.

Uncertain Successes vs Success Percentage

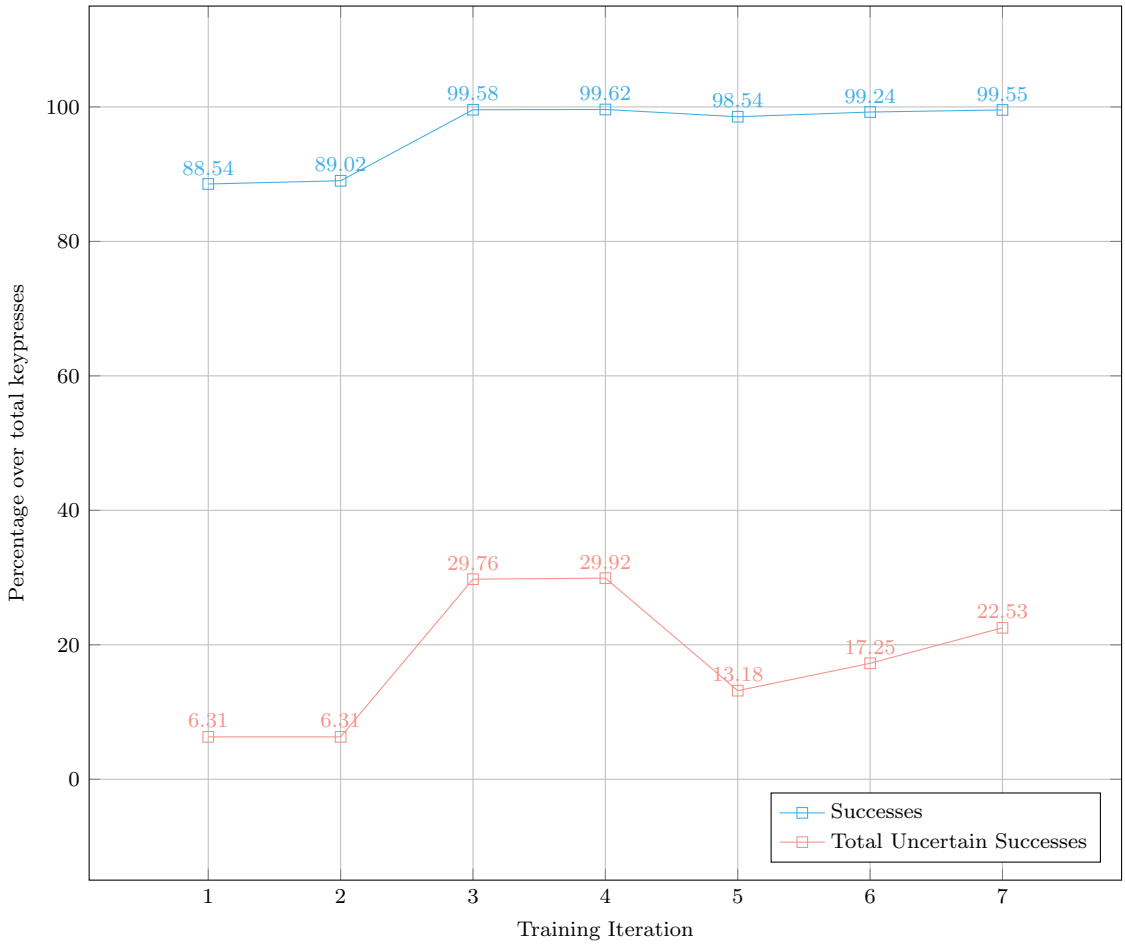

Figure 4.3: Uncertain Successes of the training iterations

Tuning the algorithm required managing both uncertain successes and the success percentage and making compromises between one or the other. The goal of the training process was to maximize the success percentage while limiting the number of uncertain successes.

As seen in Figure 4.3, it can be noted that in iterations one and two, the success rate was lower compared to the other iterations. However, the percentage of uncertain successes was also the lowest. Iteration three was the first iteration that created a buffer around each key, however, this buffer of 10 pixels was too aggressive, with the uncertain successes spiking upwards to nearly 30%. Iteration five reduced the buffer size by half to five pixels. This did not affect the success rate that much, with

only a reduction of 1.08%. This also greatly decreased the uncertain success percentage by 16.74%. The sixth iteration met halfway between iterations four and five, by adding a buffer of seven pixels. This increased the success rate back to 99.24% without greatly increasing the number of uncertain successes. In comparison with the fourth iteration, the sixth iteration had its success rate decrease by 0.38%, but its percentage of uncertain successes decreased by 12.67%. A seventh iteration was trialed where the increase in buffer was asymmetrical. For each key, the points nearer the user were increased by 10 pixels, while the points farther away were increased by five pixels only. This slightly increased the success rate by 0.31%. However, the percentage of uncertain successes also increased by 5.28%.

While the percentage of uncertain successes in iterations five through seven was in the range of 13% to 20%, The majority of these uncertain successes were spacebar uncertain successes, as shown in Figure 4.2.

Based on these results, the final selected parameters for the module were the parameters set in iteration six, with the buffer set to seven pixels as it was a good middle ground between success rate and uncertain successes.

Failure Types

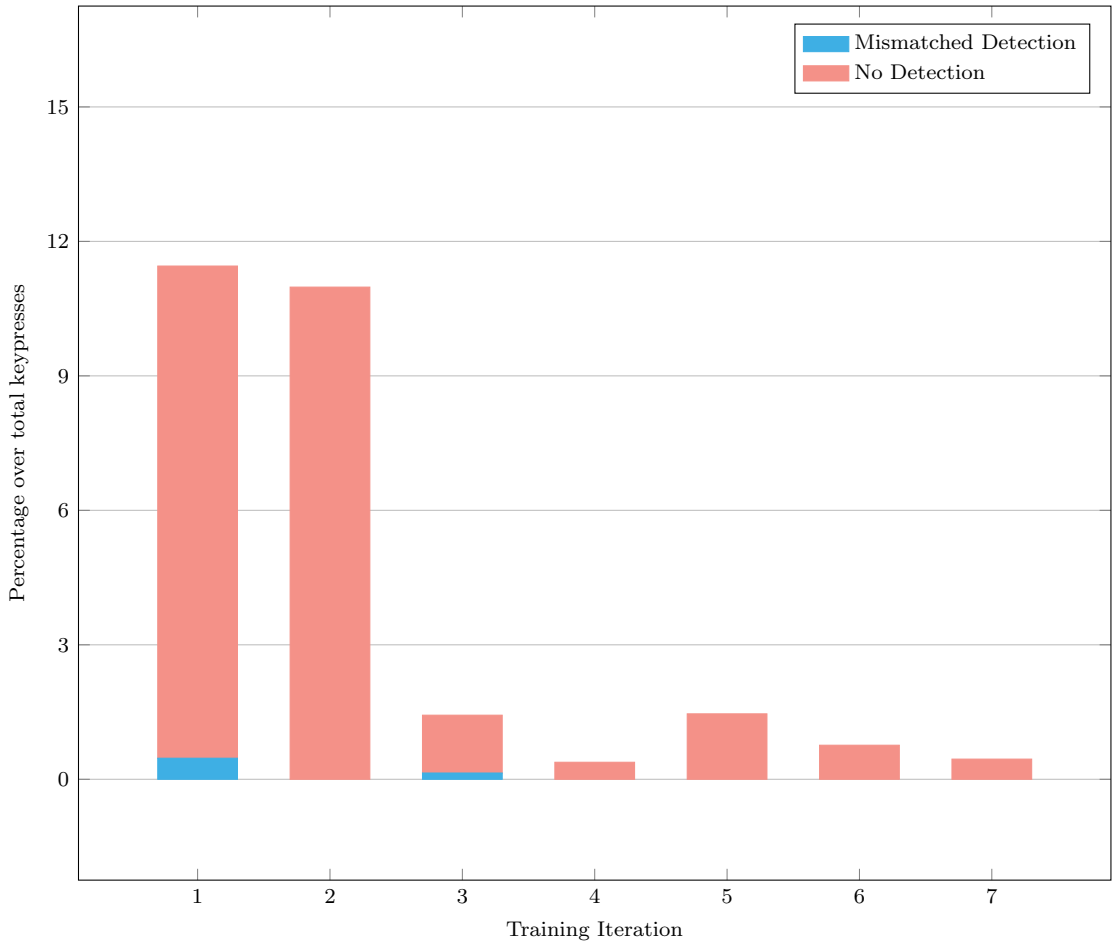

Figure 4.4: Uncertain Successes of the training iterations

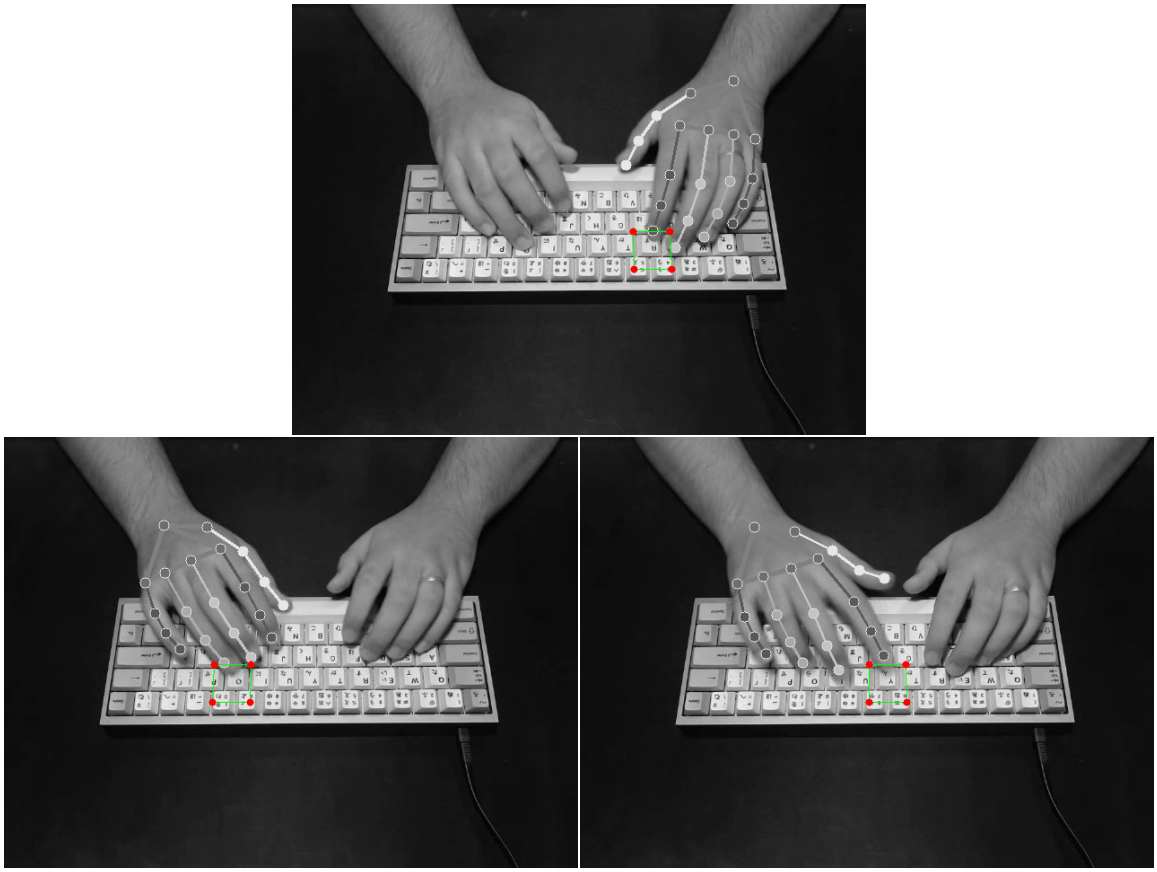

Figure 4.5: Example of No Identification Failures

Mismatched Identification These are failures where the module did not return the expected fingertip based on the manual labeling. This type of failure only manifested in iterations one and three. The failures in iteration one, after double-checking the video, were due to an error during manual labeling. In iteration three, these errors were due to an incorrect image map and Key-Color Values map. The information for some keys was not consistent between both.

Based on this information and from the gathered data as shown in Figure 4.4, this failure type is non-existent for the module in real-life conditions.

No Identification These are failures where the module did not detect any fingertips within the ROI. Figure 4.5 shows examples of frames where these errors occurred. These made up all the failures from the test results. These types of failures occurred because the fingertips used to press the key were not directly above the key, but rather offset to its side. Scaling the ROI would reduce

the number of no identification failures, but it would also increase the number of uncertain successes. See Section 4.1.1, Uncertain Successes vs Success Percentage for more information.

Occlusion

The module was also successful in finger-key identification, even if both the key and finger were occluded. Figure 4.6 is one frame where this occurred. The module was successful in identifying that the Left Thumb was used to press the Left Shift.

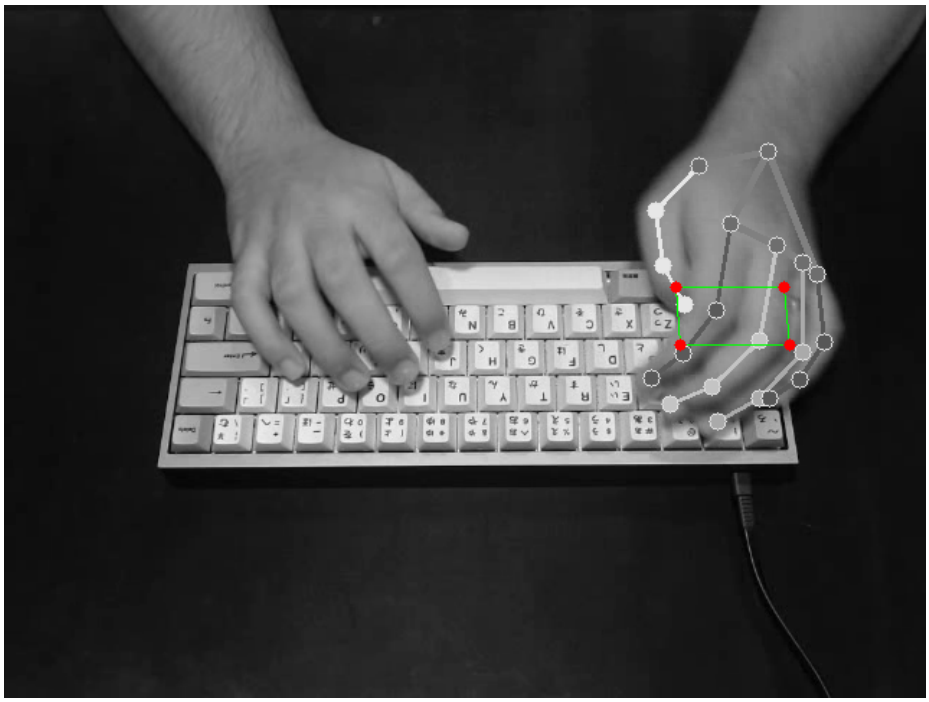

Figure 4.6: Occluded finger and key

4.1.2 Test Results

Table 4.1: Accuracy Results of the Module with Test Data

Category	Value
Total Keypresses	942
Identifications	
Successes	938
Failures	4
Success Percentage / Accuracy	99.58%
Failure Percentage	0.42%
Failure Types	
Mismatched Identification	0
No Identification	4
Uncertain Successes	
Total	133
Spacebar	72
Spacebar Percentage	54.14%
Spacebar Percentage (Total)	7.64%
Non-spacebar	61
Non-spacebar Percentage	45.86%
Non-spacebar Percentage (Total)	6.48%

Table 4.1 provides the accuracy results of the module with test data. These results were satisfactory after running the module with the parameters from the sixth training iteration on the test data. There was another run with the same test data and the same parameters, however, these results were omitted since this run had inconclusive results as there was a single identification that was incorrectly labeled during manual finger-key identification.

4.2 Speed

Based on the definition of WPM from Arif and Stuerzlinger (2009) as seen in Equation 2.1, it can be extrapolated that calculating Characters per Second (CPS) is:

$$CPS = \frac{WPM}{60} \cdot 5 \tag{4.2}$$

The average WPM when typing using the QWERTY layout, according to test data from "keybr.com - Typing lessons" is ≈ 37.5 WPM. As such, we can calculate that the average Characters per Second when typing using the QWERTY layout is 3.125. We can calculate the seconds needed per character by this equation:

$$s = \frac{1}{CPS} \tag{4.3}$$

This means that each character, on average, requires 0.32 seconds to type. This sets the maximum time spent for finger-key identification for a single character. Any more than this would result in a noticeable slowdown during typing.

4.2.1 Results

Training Iterations

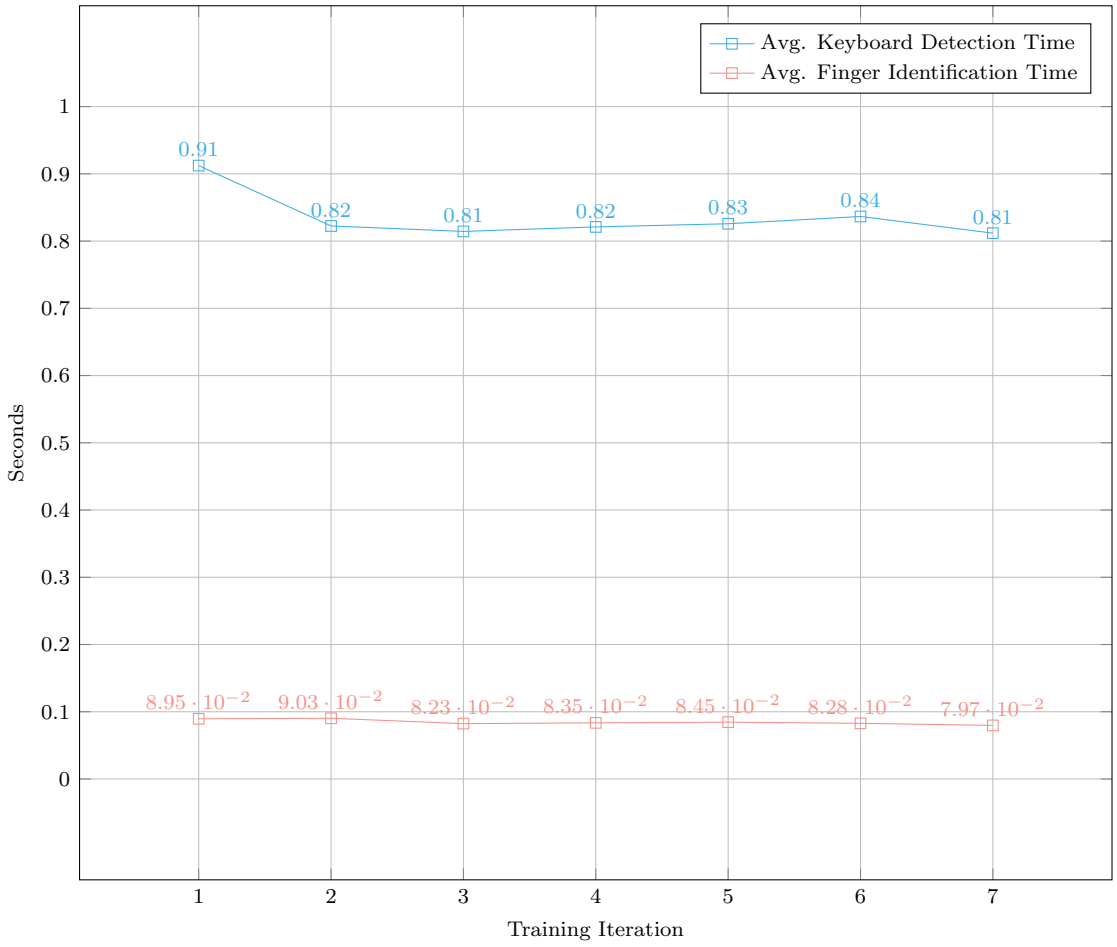

Figure 4.7: Keyboard detection time of the training iterations

The training iterations had an average keyboard detection time of $0.8620 \pm 0.0502s$ and average finger identification time of $0.0863 \pm 0.0040s$. Throughout the training, there was no noticeable difference in running time over the same dataset as shown in Figure 4.7. However, the first training iteration had issues with gathering the speed of the module, as the average keyboard detection time included other operations that were not part of getting the Key-Edge Coordinates Map. Removing this iteration, the average keyboard detection time becomes more consistent, with it being $0.8295 \pm 0.0070s$.

Test Results

Table 4.2: Speed Results of the Module with Test Data

Category	Seconds
Avg. Keyboard Detection Time	0.838
Avg. Finger Identification Time	0.083

These results, as tabulated in Table 4.2 were consistent with the training iterations. This means that the module has repeatable and predictable running times.

4.2.2 Average Keyboard Detection Time

This is the time that was measured as the module generated the Key-Edge Coordinates Map. This corresponds with the first step of the module. It is to be noted that this time does not affect keyboard typing and is not limited by the 0.32 threshold as the user is not yet typing at this point.

4.2.3 Average Finger Identification Time

This is the time spent in finger-key identification for a single key. As such, this time should be below 0.32 seconds for the module to be capable of performing finger-key identification in real-time without noticeable slowdown from the perspective of the user.

The average finger identification time that the module got was 0.083s which is well below 0.32s. This can be attributed to the speed of the MediaPipe library, and the pre-calculation of the edge coordinates.

Real-Time Finger-Key Identification

With each keypress only requiring 0.083s for finger-key identification, it can be gathered that the maximum CPS which the module can still perform real-time finger-key identification is 11.9200 CPS, based on Equation 4.3. It follows that the maximum WPM that still allows for real-time finger-key identification is 143.040 WPM, based on Equation 4.2. This is well above the median of 37.5 WPM on Keybr. The module can also perform finger-key identification for 90.99% of the community members of Monkeytype with the speed role.

Chapter 5

Conclusion

The finger key identification module was successfully developed and implemented in this study.

The finger-key identification solution was split into two parts, keyboard detection and key mapping, and finger detection. Keyboard detection and key mapping used the following algorithm and techniques: (1) Edge Detection using Sobel filter (Sobel, 2014), (2) Thresholding using Otsu's algorithm (Otsu, 1979), (3) Finding contours using the algorithm of Suzuki and Abe (1985), (4) Line Simplification using the Douglas-Peucker algorithm (Saalfeld, 1999), and (5) Perspective transform ("OpenCV: Geometric Image Transformations," n.d.). Finger detection utilized a ready-made solution called MediaPipe Hands by Lugaresi et al. (2019). The two were combined to perform finger-key identification.

The keyboard used was a 60% keyboard in ANSI. It was light in color and was connected with a black USB-C cable. The surface of the desk was dark, and a LED Bulb rated at 9 Watts, 700 lumens, and 6500k color temperature was used to uniformly light the capture area. The single optical camera, a Logitech C920, was placed above the keyboard, pointing directly downwards. It captured videos in 720p/30fps with a diagonal field of view of 78°("Logitech C920 PRO HD Webcam, 1080p Video with Stereo Audio," n.d.). The computer used had an AMD Ryzen 5 3600 CPU, AMD Radeon RX 5600 XT GPU, G.Skill Trident Z Neo RGB 16GB 3200mhz RAM, and Samsung SSD 850 EVO SSD.

The development of the module utilized OpenCV as the main image manipulation platform that implemented the algorithms mentioned previously. OpenCV was also used to capture videos from the optical camera. It was all written in Python.

The module was accurate in 99.58% of identifications in a data set composed of 942 keypresses.

However, 14.12% of the identifications were uncertain successes. These are successes where more than one fingertip was found in an ROI. Of these, 6.48% were non-spacebar uncertain successes. These are uncertain successes over keys that are not the spacebar. This bears more weight since most of these keys are the smallest on the keyboard, and in most cases, only one fingertip could fit within the key. These uncertain successes were due to the addition of a buffer around each ROI to increase the success rate.

The module is fast enough for real-time finger-key identification up to typing speeds of 143.040 WPM. This is above the median typing speed of 37.5 WPM on Keybr ("keybr.com - Typing lessons," 2021). This also handles 90.99% of the 12678 members with the speed role on MonkeyType (Bartnik, 2022).

Two metrics were developed and implemented in a proof of concept trainer: (1) Finger Placement Accuracy which computes the percentage of keys pressed with the correct figure over the length of the test sequence, and (2) Historical Finger Placement Accuracy which computes the number of times the user is successful if pressing a key with the correct finger over all test sequences.

Chapter 6

Future Work

6.1 Trainer

A proof of concept trainer with real-time finger-key identification was developed, however this trainer is lacking in functionality to be an actual usable trainer that will be used for educational purposes.

In addition, the wall of latency that exists during th Key-Edge Coordinates Map can be removed by doing this process on the browser. This can be done by redoing the process in C, and compiling that to WebAssembly. The MediaPipe team did the same thing for MediaPipe Hands, and performance, for this use case, was more or less equal.

6.2 Standardized Finger-Key Mapping

While there are mappings for the default ANSI and ISO layouts, these layouts were not official and were defacto standards. While the trainer uses this defacto standard, it wouldn't be difficult to adapt the trainer to use another standard for finger-key mapping.

6.3 Character Representation

The test and training data did not have equal representation of the keys within the keyboard. For the module to undergo more rigorous testing, it would be better to have a dataset that has equal

representation of all of the characters in the keyboard.

6.4 Effects on Touch Typing Education

The paper created a method for finger-key identification in hopes of improving touch typing education, however, there was no test done to prove that the module will affect the learner's skill in touch typing

6.5 Effects on Health

In connection with the previous section, the module also has no testing done to quantify if training using the module will improve the posture and reduce problematic hand positions and movements that can cause nerve and muscular disorders.

6.6 Environmental Setup

The environmental setup was tightly controlled, with the keyboard and the desk of contrasting color, lighting was nearly perfect, and the camera was of great quality. This is not realistic and is not representative of the real world. Future work could improve upon this area. An idea would be to have a separate process where the user could just select four points rather than relying on an automated computer vision process to detect the four edges.

6.7 ROI Buffer

The buffer was selected after trail and error in the training phase of the algorithm. However, this buffer may not be the best and adaptive techniques or a machine learning algorithm may select better values for the buffer.

6.8 Detecting Keyboard Movement Between Frames

The module is limited in its ability to track keyboards that move between keypresses. While this is not something that usually happens during keyboard typing, having the ability to track movements would be a great addition to improving the module's performance.

6.9 Different Keyboard Types, Layouts, and Colors

The module is limited to detecting keypresses with a 60% keyboard. This type of keyboard is not that commonly used. Other keyboard types, like the 100%, 75%, and TKLs would be good starting points for adding support. In addition, supporting other layouts, like ISO, would also greatly increase the number of people that could use the module. Furthermore, supporting other color schemes would also widen the number of keyboards that can be used with the module.

Chapter A
Key-Color Values Map

Key	Color (in BGR)
LeftControl	(85, 0, 0)
LeftSuper	(45, 0, 0)
LeftAlt	(58, 35, 0)
Spacebar	(62, 55, 0)
RightAlt	(0, 28, 44)
RightSuper	(0, 3, 73)
RightControl	(24, 0, 76)
‘	(255, 0, 0)
1	(255, 153, 0)
2	(255, 229, 0)
3	(189, 255, 0)
4	(143, 255, 0)
5	(51, 255, 0)
6	(0, 255, 102)
7	(0, 255, 194)
8	(0, 224, 255)
9	(0, 163, 255)
0	(0, 102, 255)
-	(0, 10, 255)
=	(82, 0, 255)
|	(128, 0, 255)
Delete	(189, 0, 255)
Tab	(224, 0, 0)

Continued on next column

Key	Color (in BGR)
Q	(214, 128, 0)
W	(225, 203, 0)
E	(160, 217, 0)
R	(126, 224, 0)
T	(43, 217, 0)
Y	(0, 216, 86)
U	(0, 195, 149)
I	(0, 183, 208)
O	(0, 136, 212)
P	(0, 79, 196)
]	(0, 8, 211)
[	(63, 0, 196)
Backspace	(134, 0, 181)
CapsLock	(195, 0, 0)
A	(167, 100, 0)
S	(178, 161, 0)
D	(124, 168, 0)
F	(101, 180, 0)
G	(31, 157, 0)
H	(0, 139, 56)
J	(1, 139, 106)
K	(0, 130, 148)
L	(0, 94, 147)

Continued on next column

Key	Color (in BGR)
;	(0, 52, 130)
’	(0, 7, 170)
Enter	(35, 0, 109)
LeftShift	(150, 0, 0)
Z	(104, 62, 0)
X	(130, 117, 0)
C	(77, 104, 0)
V	(63, 113, 0)
B	(18, 88, 0)
N	(0, 66, 26)
M	(0, 84, 64)
,	(0, 75, 85)
.	(0, 70, 109)
/	(0, 32, 80)
RightShift	(0, 5, 128)

Concluded

Chapter B

Typing Test Sequences

1. “What of it, if some old hunks of a sea-captain orders me to get a broom and sweep down the decks?” (Melville, 2001)
2. “I sat down on an old wooden settle, carved all over like a bench on the Battery.” (Melville, 2001)
3. “I lay there dismally calculating that sixteen entire hours must elapse before I could hope for a resurrection.” (Melville, 2001)
4. “How slowly the time passes here, encompassed as I am by frost and snow!” (Shelley, 1993)
5. “I listened to my father in silence and remained for some time incapable of offering any reply.” (Shelley, 1993)
6. “Think you’re escaping and run into yourself. Longest way round is the shortest way home.” (Joyce, 2003)
7. “History, Stephen said, is a nightmare from which I am trying to awake” (Joyce, 2003)
8. “A man of genius makes no mistakes. His errors are volitional and are the portals of discovery.” (Joyce, 2003)
9. “Never trust to general impressions, my boy, but concentrate yourself upon details” (Doyle, 1999)
10. “I have no data yet. It is a capital mistake to theorise before one has data.” (Doyle, 1999)

Chapter C

Screenshots of Data Analysis

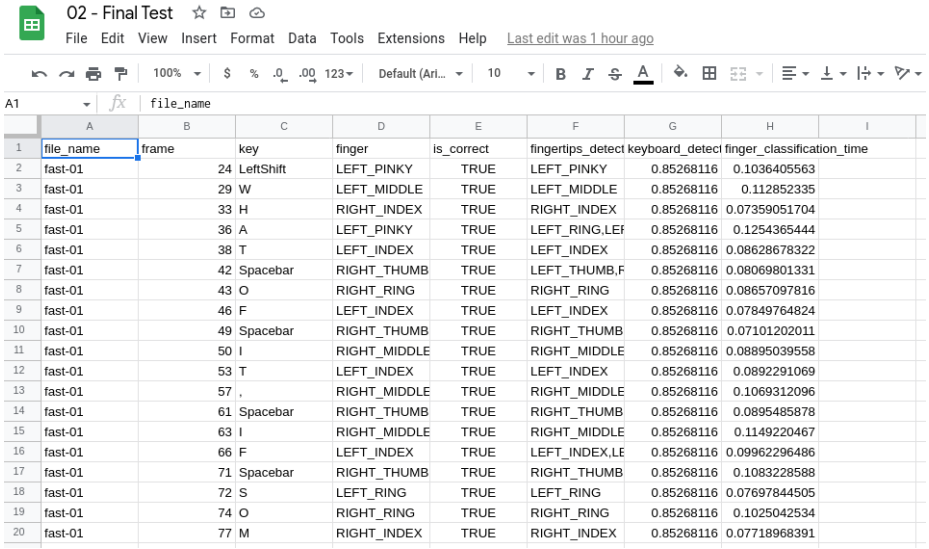

	A	B	C	D	E	F	G	H	I
1	file_name	frame	key	finger	is_correct	fingertips_detect	keyboard_detect	finger_classification_time	
2	fast-01	24	LeftShift	LEFT_PINKY	TRUE	LEFT_PINKY	0.85268116	0.1036405563	
3	fast-01	29	W	LEFT_MIDDLE	TRUE	LEFT_MIDDLE	0.85268116	0.112852335	
4	fast-01	33	H	RIGHT_INDEX	TRUE	RIGHT_INDEX	0.85268116	0.07359051704	
5	fast-01	36	A	LEFT_PINKY	TRUE	LEFT_RING,LEF	0.85268116	0.1254365444	
6	fast-01	38	T	LEFT_INDEX	TRUE	LEFT_INDEX	0.85268116	0.08628678322	
7	fast-01	42	Spacebar	RIGHT_THUMB	TRUE	LEFT_THUMB,F	0.85268116	0.08069801331	
8	fast-01	43	O	RIGHT_RING	TRUE	RIGHT_RING	0.85268116	0.08657097816	
9	fast-01	46	F	LEFT_INDEX	TRUE	LEFT_INDEX	0.85268116	0.07849764824	
10	fast-01	49	Spacebar	RIGHT_THUMB	TRUE	RIGHT_THUMB	0.85268116	0.07101202011	
11	fast-01	50	I	RIGHT_MIDDLE	TRUE	RIGHT_MIDDLE	0.85268116	0.08895039558	
12	fast-01	53	T	LEFT_INDEX	TRUE	LEFT_INDEX	0.85268116	0.0892291069	
13	fast-01	57	,	RIGHT_MIDDLE	TRUE	RIGHT_MIDDLE	0.85268116	0.1069312096	
14	fast-01	61	Spacebar	RIGHT_THUMB	TRUE	RIGHT_THUMB	0.85268116	0.0895485878	
15	fast-01	63	I	RIGHT_MIDDLE	TRUE	RIGHT_MIDDLE	0.85268116	0.1149220467	
16	fast-01	66	F	LEFT_INDEX	TRUE	LEFT_INDEX,LE	0.85268116	0.09962296486	
17	fast-01	71	Spacebar	RIGHT_THUMB	TRUE	RIGHT_THUMB	0.85268116	0.1083228588	
18	fast-01	72	S	LEFT_RING	TRUE	LEFT_RING	0.85268116	0.07697844505	
19	fast-01	74	O	RIGHT_RING	TRUE	RIGHT_RING	0.85268116	0.1025042534	
20	fast-01	77	M	RIGHT_INDEX	TRUE	RIGHT_INDEX	0.85268116	0.07718968391	

Figure C.1: Raw data as seen on Google Sheets

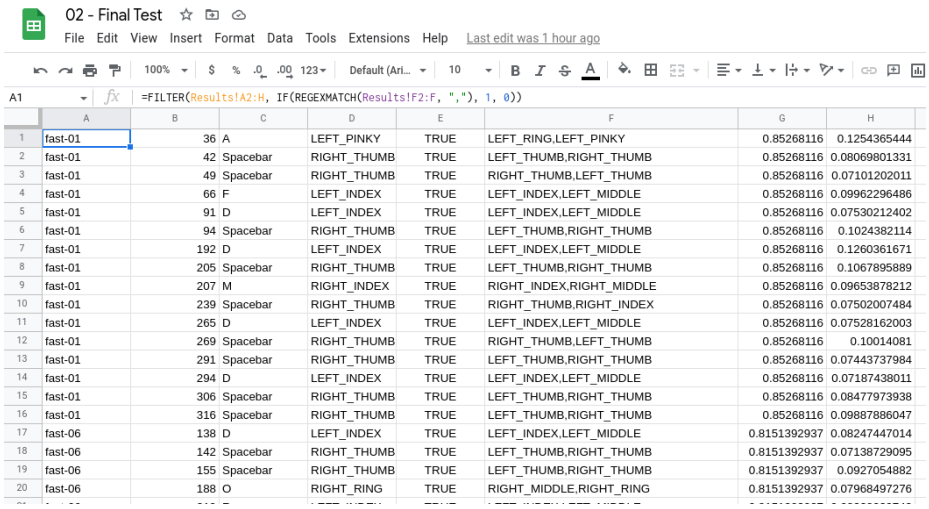

	A	B	C	D	E	F	G	H
1	fast-01	36	A	LEFT_PINKY	TRUE	LEFT_RING,LEFT_PINKY	0.85268116	0.1254365444
2	fast-01	42	Spacebar	RIGHT_THUMB	TRUE	LEFT_THUMB,RIGHT_THUMB	0.85268116	0.08069801331
3	fast-01	49	Spacebar	RIGHT_THUMB	TRUE	RIGHT_THUMB,LEFT_THUMB	0.85268116	0.07101202011
4	fast-01	66	F	LEFT_INDEX	TRUE	LEFT_INDEX,LEFT_MIDDLE	0.85268116	0.09962296486
5	fast-01	91	D	LEFT_INDEX	TRUE	LEFT_INDEX,LEFT_MIDDLE	0.85268116	0.07530212402
6	fast-01	94	Spacebar	RIGHT_THUMB	TRUE	LEFT_THUMB,RIGHT_THUMB	0.85268116	0.1024382114
7	fast-01	192	D	LEFT_INDEX	TRUE	LEFT_INDEX,LEFT_MIDDLE	0.85268116	0.1260361671
8	fast-01	205	Spacebar	RIGHT_THUMB	TRUE	LEFT_THUMB,RIGHT_THUMB	0.85268116	0.1067895889
9	fast-01	207	M	RIGHT_INDEX	TRUE	RIGHT_INDEX,RIGHT_MIDDLE	0.85268116	0.09653878212
10	fast-01	239	Spacebar	RIGHT_THUMB	TRUE	RIGHT_THUMB,RIGHT_INDEX	0.85268116	0.07502007484
11	fast-01	265	D	LEFT_INDEX	TRUE	LEFT_INDEX,LEFT_MIDDLE	0.85268116	0.07528162003
12	fast-01	269	Spacebar	RIGHT_THUMB	TRUE	RIGHT_THUMB,LEFT_THUMB	0.85268116	0.10014081
13	fast-01	291	Spacebar	RIGHT_THUMB	TRUE	LEFT_THUMB,RIGHT_THUMB	0.85268116	0.07443737984
14	fast-01	294	D	LEFT_INDEX	TRUE	LEFT_INDEX,LEFT_MIDDLE	0.85268116	0.07187438011
15	fast-01	306	Spacebar	RIGHT_THUMB	TRUE	LEFT_THUMB,RIGHT_THUMB	0.85268116	0.08477973938
16	fast-01	316	Spacebar	RIGHT_THUMB	TRUE	LEFT_THUMB,RIGHT_THUMB	0.85268116	0.09887886047
17	fast-06	138	D	LEFT_INDEX	TRUE	LEFT_INDEX,LEFT_MIDDLE	0.8151392937	0.08247447014
18	fast-06	142	Spacebar	RIGHT_THUMB	TRUE	LEFT_THUMB,RIGHT_THUMB	0.8151392937	0.07138729095
19	fast-06	155	Spacebar	RIGHT_THUMB	TRUE	LEFT_THUMB,RIGHT_THUMB	0.8151392937	0.0927054882
20	fast-06	188	O	RIGHT_RING	TRUE	RIGHT_MIDDLE,RIGHT_RING	0.8151392937	0.07968497276

Figure C.2: Filtered raw data to show uncertain successes

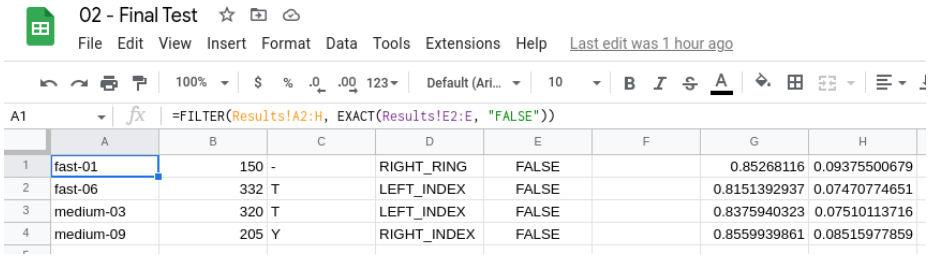

	A	B	C	D	E	F	G	H
1	fast-01	150	-	RIGHT_RING	FALSE		0.85268116	0.09375500679
2	fast-06	332	T	LEFT_INDEX	FALSE		0.8151392937	0.07470774651
3	medium-03	320	T	LEFT_INDEX	FALSE		0.8375940323	0.07510113716
4	medium-09	205	Y	RIGHT_INDEX	FALSE		0.8559939861	0.08515977859

Figure C.3: Filtered raw data to show failures

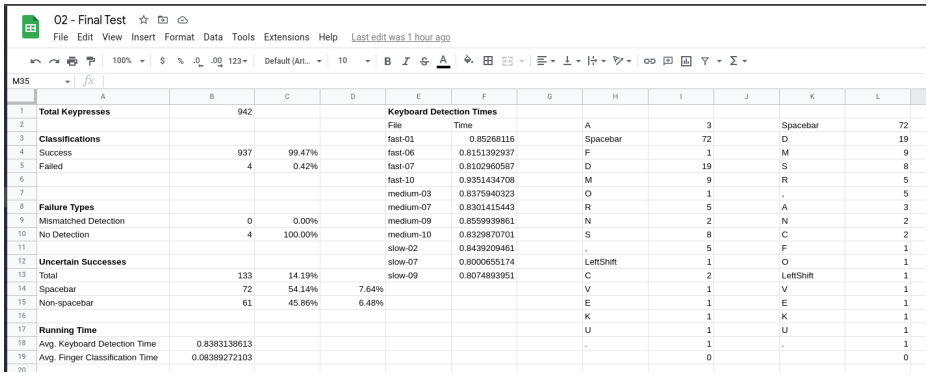

	A	B	C	D	E	F	G	H	I	J	K	L
1	**Total Keypresses**	942			**Keyboard Detection Times**							
2					File	Time		A	3		Spacebar	72
3	**Classifications**				fast-01	0.85268116		Spacebar	72		D	19
4	Success	937	99.47%		fast-06	0.8151392937		F	1		M	9
5	Failed	4	0.42%		fast-07	0.8102960587		D	19		S	8
6					fast-10	0.9351434708		M	9		R	5
7					medium-03	0.8375940323		O	1		.	5
8	**Failure Types**				medium-07	0.8301415443		R	5		A	3
9	Mismatched Detection	0	0.00%		medium-09	0.8559939861		N	2		N	2
10	No Detection	4	100.00%		medium-10	0.8329870701		S	8		C	2
11					slow-02	0.8439209461		,	5		F	1
12	**Uncertain Successes**				slow-07	0.8000655174		LeftShift	1		O	1
13	Total	133	14.19%		slow-09	0.8074893951		C	2		LeftShift	1
14	Spacebar	72	54.14%	7.64%				V	1		V	1
15	Non-spacebar	61	45.86%	6.48%				E	1		E	1
16								K	1		K	1
17	**Running Time**							U	1		U	1
18	Avg. Keyboard Detection Time	0.8383138613						.	1		.	1
19	Avg. Finger Classification Time	0.08389272103							0			0

Figure C.4: Metrics calculated from the raw data

Chapter D

Gantt Chart

Development of a touch typing trainer with an emphasis on finger-key identification

Oscar Vian L. Valles

Project Start Date: 2/21/2022 (Monday) Display Week: 1

WBS	Task	Start	End	Days	% Done	Work Days
1	**Experimental Setup**	Mon 2/21/22	Mon 2/21/22	1		1
1.1	Camera Setup and Placement	Mon 2/21/22	Mon 2/21/22	1	0%	1
1.2	Keyboard Setup and Placement	Mon 2/21/22	Mon 2/21/22	1	0%	1
1.3	Environmental Setup and Placement	Mon 2/21/22	Mon 2/21/22	1	0%	1
2	**Keyboard Detection and Mapping**	Tue 2/22/22	Fri 3/18/22	25		19
2.1	Convert to Greyscale and Edge Detection using Sobel Filter	Tue 2/22/22	Sat 3/05/22	12	0%	9
2.2	Find Contours	Mon 3/07/22	Fri 3/11/22	5	0%	5
2.3	Overlay Virtual Keyboard Map	Mon 3/14/22	Tue 3/15/22	2	0%	2
2.4	Methodology Writing	Wed 3/16/22	Fri 3/18/22	3	0%	3
3	**Finger Detection and Tracking, Integration**	Mon 3/21/22	Wed 4/13/22	24		18
3.1	Finger Detection and Tracking	Mon 3/21/22	Fri 3/25/22	5	0%	5
3.2	Integration (Find ROI)	Mon 3/28/22	Fri 4/01/22	5	0%	5
3.3	Integration (Find and Return Fingertip on ROI)	Mon 4/04/22	Fri 4/08/22	5	0%	5
3.4	Methodology Writing	Mon 4/11/22	Wed 4/13/22	3	0%	3
4	**Touch Typing Trainer**	Thu 4/14/22	Thu 5/19/22	36		26
4.1	Front-end Development	Thu 4/14/22	Sat 4/23/22	10	0%	7
4.2	Back-end Development	Sun 4/24/22	Tue 5/03/22	10	0%	7
4.3	Finger-key Identification and Mapping Accuracy	Wed 5/04/22	Fri 5/13/22	10	0%	8
4.4	Methodology, Results and Discussion Writing	Sat 5/14/22	Thu 5/19/22	6	0%	4
5	**Final Paper Writing and Presentation**	Fri 5/20/22	Wed 6/15/22	27		19
5.1	Conclusion	Fri 5/20/22	Sun 5/22/22	3	0%	1
5.2	Recommendation and Future Work	Mon 5/23/22	Wed 5/25/22	3	0%	3
5.3	Proofreading	Thu 5/26/22	Fri 6/03/22	9	0%	7
5.4	Journal Article Writing	Sat 6/04/22	Fri 6/10/22	7	0%	5
5.5	Presentation Preparation	Sat 6/11/22	Wed 6/15/22	5	0%	3

References

About TypeRacer. (2021). Retrieved October 26, 2021, from https://data.typeracer.com/misc/about

Alexanderson, S., O'Sullivan, C., & Beskow, J. (2016). Robust online motion capture labeling of finger markers. *Proceedings of the 9th International Conference on Motion in Games*, 7–13. https://doi.org/10.1145/2994258.2994264

ANSI INCITS 154-1988. (1999). *Office Machines and Supplies - Alphanumeric Machines - Keyboard Arrangement* (Standard). American National Standards Institute. Washington, D.C., USA.

Apple. (2021). How to identify your Apple keyboard layout by country or region. Retrieved October 18, 2021, from https://support.apple.com/en-ph/HT201794

Arif, A., & Stuerzlinger, W. (2009). Analysis of text entry performance metrics, 100–105. https://doi.org/10.1109/TIC-STH.2009.5444533

Baker, N., Cham, R., Cidboy, E., Cook, J., & Redfern, M. (2007). Kinematics of the fingers and hands during computer keyboard use. *Clinical Biomechanics*, *22*(1), 34–43. https://doi.org/10.1016/j.clinbiomech.2006.08.008

Baker, N., Cham, R., Hale, E., Cook, J., & Redfern, M. (2007). Digit kinematics during typing with standard and ergonomic keyboard configurations. *International Journal of Industrial Ergonomics*, *37*(4), 345–355. https://doi.org/10.1016/j.ergon.2006.12.004

Bartnik, J. (2021). https://monkeytype.com/about

Bartnik, J. (2022). Monkey-Stats.

Bradski, G. (2000). The OpenCV Library. *Dr. Dobb's Journal of Software Tools*.

Ciobanu, O., Gavat, C., & Cozmei, R. (2016). The keyboard remains the least economically designed computer device. https://doi.org/10.1109/EHB.2015.7391585

Common Core State Standards Initiative (CCSS). (2010). *Common core state standards for English Language Arts & Literacy in History/Social Studies, Science, and Technical Subjucts* (tech. rep.). Retrieved October 26, 2021, from http://www.corestandards.org/wp-content/uploads/ELA_Standards1.pdf

Department of Education. (2020). *Contextualized Mechanisms to guide Schools in the implementation of the Blended/Distance Learning Delivery Modality* (tech. rep.). Retrieved October 26, 2021, from https://www.depedcar.ph/sites/default/files/regionalMemos/long-memo_1.pdf

Dobson, A. (2009). *Touch Typing in Ten Hours*. Hachette UK.

Donica, D. K., Giroux, P., & Faust, A. (2018). Keyboarding instruction: Comparison of techniques for improved keyboarding skills in elementary students. *Journal of Occupational Therapy, Schools, & Early Intervention*, *11*(4), 396–410. https://doi.org/10.1080/19411243.2018.1512067

Dorfmuller-Ulhaas, K., & Schmalstieg, D. (2001). Finger tracking for interaction in augmented environments. *Proceedings IEEE and ACM International Symposium on Augmented Reality*, 55–64. https://doi.org/10.1109/ISAR.2001.970515

Doyle, A. C. (1999). *The Adventures of Sherlock Holmes*. Retrieved February 3, 2022, from https://www.gutenberg.org/ebooks/1661

DraugTheWhopper. (2014). MS Natural Multimedia Keyboard. Retrieved October 28, 2021, from https://commons.wikimedia.org/wiki/File:MS_Natural_Multimedia_Keyboard.png

Ergodox EZ. (n.d.). ErgoDox EZ: An Incredible Mechanical Ergonomic Keyboard. Retrieved October 28, 2021, from https://ergodox-ez.com/

Fisher, B. (n.d.). Bilateral Filtering. Retrieved May 18, 2022, from https://homepages.inf.ed.ac.uk/rbf/CVonline/LOCAL_COPIES/MANDUCHI1/Bilateral_Filtering.html

Gerr, F., Marcus, M., Ensor, C., Kleinbaum, D., Cohen, S., Edwards, A., Gentry, E., Ortiz, D., & Monteilh, C. (2002). A prospective study of computer users: I. Study design and incidence of musculoskeletal symptoms and disorders. *American Journal of Industrial Medicine*, *41*(4), 221–235. https://doi.org/10.1002/ajim.10066

Halder, A., & Tayade, A. (2021). Real-time vernacular sign language recognition using mediapipe and machine learning. *International Journal of Research Publication and Reviews*, *2582*.

Hoot, J. L. (1986). Keyboarding Instruction in the Early Grades: Must or Mistake? [Publisher: Routledge _eprint: https://doi.org/10.1080/00094056.1986.10521749]. *Childhood Education*, *63*(2), 95–101. https://doi.org/10.1080/00094056.1986.10521749

Hsu, M. H., Shih, T. K., & Chiang, J. S. (2014). Real-Time Finger Tracking for Virtual Instruments. *2014 7th International Conference on Ubi-Media Computing and Workshops*, 133–138. https://doi.org/10.1109/U-MEDIA.2014.53

Huang, T. (1996). Computer Vision : Evolution And Promise [Publisher: CERN]. https://doi.org/10.5170/CERN-1996-008.21

ISO/IEC 9995-1:2009. (2016). *Information technology — Keyboard layouts for text and office systems* (Standard). International Organization for Standardization.

Joyce, J. (2003). *Ulysses*. Retrieved February 3, 2022, from https://www.gutenberg.org/ebooks/4300

Keyboarding Without Tears — K-5. (2020). Retrieved October 26, 2021, from https://issuu.com/handwritingwithouttears/docs/kwtbrochure2020/1

Keybr.com - Typing lessons. (2021). Retrieved October 26, 2021, from http://www.keybr.com/

Liu, W., Anguelov, D., Erhan, D., Szegedy, C., Reed, S., Fu, C.-Y., & Berg, A. C. (2016). SSD: Single Shot MultiBox Detector [arXiv: 1512.02325]. *arXiv:1512.02325 [cs]*. https://doi.org/10.1007/978-3-319-46448-0_2

Logan, G., Ulrich, J., & Lindsey, D. (2016). Different (key)strokes for different folks: How standard and nonstandard typists balance Fitts' law and Hick's law. *Journal of Experimental Psychology: Human Perception and Performance*, *42*(12), 2084–2102. https://doi.org/10.1037/xhp0000272

Logitech C920 PRO HD Webcam, 1080p Video with Stereo Audio. (n.d.). Retrieved January 26, 2022, from https://www.logitech.com/en-ph/products/webcams/c920-pro-hd-webcam.html

Lugaresi, C., Tang, J., Nash, H., McClanahan, C., Uboweja, E., Hays, M., Zhang, F., Chang, C.-L., Yong, M., Lee, J., Chang, W.-T., Hua, W., Georg, M., & Grundmann, M. (n.d.). Hands. Retrieved January 13, 2022, from https://google.github.io/mediapipe/solutions/hands.html

Lugaresi, C., Tang, J., Nash, H., McClanahan, C., Uboweja, E., Hays, M., Zhang, F., Chang, C.-L., Yong, M., Lee, J., Chang, W.-T., Hua, W., Georg, M., & Grundmann, M. (2019). MediaPipe: A Framework for Perceiving and Processing Reality. *Third Workshop on Computer Vision for AR/VR at IEEE Computer Vision and Pattern Recognition (CVPR) 2019*. https://mixedreality.cs.cornell.edu/s/NewTitle_May1_MediaPipe_CVPR_CV4ARVR_Workshop_2019.pdf

Marklin, R. W., Simoneau, G. G., & Monroe, J. F. (1999). Wrist and forearm posture from typing on split and vertically inclined computer keyboards. *Human Factors*, *41*(4), 559–569. https://doi.org/10.1518/001872099779656770

MathWorks. (2021a). Computer Vision Toolbox. Retrieved October 28, 2021, from https://www.mathworks.com/products/computer-vision.html

MathWorks. (2021b). What Is MATLAB? Retrieved October 28, 2021, from https://www.mathworks.com/discovery/what-is-matlab.html

Melville, H. (2001). *Moby Dick; Or, The Whale*. Retrieved December 7, 2021, from https://www.gutenberg.org/ebooks/2701

Norman, D. A., & Fisher, D. (1982). Why Alphabetic Keyboards Are Not Easy To Use: Keyboard Layout Doesn't Much Matter. *Human Factors*, *24*(5), 509–519. https://doi.org/10.1177/001872088202400502

OpenCV: Color Space Conversions. (n.d.). Retrieved May 18, 2022, from https://docs.opencv.org/4.5.5/d8/d01/group__imgproc__color__conversions.html

OpenCV: Contours : Getting Started. (n.d.). Retrieved December 14, 2021, from https://docs.opencv.org/3.4/d4/d73/tutorial_py_contours_begin.html

OpenCV: Geometric Image Transformations. (n.d.). Retrieved May 18, 2022, from https://docs.opencv.org/4.5.5/da/d54/group__imgproc__transform.html

OpenCV: Image Filtering. (n.d.). Retrieved May 18, 2022, from https://docs.opencv.org/4.5.5/d4/d86/group__imgproc__filter.html#ga9d7064d478c95d60003cf839430737ed

Operations, V. (2021). Does Typing Cause Carpal Tunnel? 3 Myths About Carpal Tunnel Syndrome. Retrieved October 26, 2021, from https://minnesotavalleysurgerycenter.com/pain-management/does-typing-cause-carpal-tunnel-3-myths-about-carpal-tunnel-syndrome/

Otsu, N. (1979). A Threshold Selection Method from Gray-Level Histograms [Conference Name: IEEE Transactions on Systems, Man, and Cybernetics]. *IEEE Transactions on Systems, Man, and Cybernetics*, *9*(1), 62–66. https://doi.org/10.1109/TSMC.1979.4310076

Parkkinen, T. (2018). The ultimate guide to keyboard layouts and form factors [Section: Keyboard Information]. Retrieved October 18, 2021, from https://blog.wooting.nl/the-ultimate-guide-to-keyboard-layouts-and-form-factors/

Poole, D., & Preciado, M. (2016). Touch typing instruction: Elementary teachers' beliefs and practices. *Computers and Education*, *102*, 1–14. https://doi.org/10.1016/j.compedu.2016.06.008

Ripat, J., Giesbrecht, E., Quanbury, A., & Kelso, S. (2010). Effectiveness of an ergonomic keyboard for typists with work related upper extremity disorders: A follow-up study. *Work*, *37*(3), 275–283. https://doi.org/10.3233/WOR-2010-1079

Rumudiez. (2013). Correctly labeled modifier keys for the ANSI Keyboard layout. Retrieved October 18, 2021, from https://commons.wikimedia.org/wiki/File:ANSI_Keyboard_Layout_Diagram_with_Form_Factor.svg

Saalfeld, A. (1999). Topologically Consistent Line Simplification with the Douglas-Peucker Algorithm [Publisher: Taylor & Francis _eprint: https://doi.org/10.1559/152304099782424901].

Cartography and Geographic Information Science, *26*(1), 7–18. https://doi.org/10.1559/152304099782424901

Serina, E. R., Tal, R., & Rempel, D. (1999). Wrist and forearm postures and motions during typing. *Ergonomics*, *42*(7), 938–951. https://doi.org/10.1080/001401399185225

Shelley, M. W. (1993). *Frankenstein; Or, The Modern Prometheus*. Retrieved February 3, 2022, from https://www.gutenberg.org/ebooks/84

Sobel, I. (2014). An Isotropic 3x3 Image Gradient Operator. *Presentation at Stanford A.I. Project 1968*.

Sung, G., Sokal, K., Uboweja, E., Bazarevsky, V., Baccash, J., Bazavan, E. G., Chang, C.-L., & Grundmann, M. (2021). *On-device Real-time Hand Gesture Recognition* (tech. rep. arXiv:2111.00038) [arXiv:2111.00038 [cs] type: article]. arXiv. https://doi.org/10.48550/arXiv.2111.00038

Suzuki, S., & Abe, K. (1985). Topological structural analysis of digitized binary images by border following. *Computer Vision, Graphics, and Image Processing*, *30*(1), 32–46. https://doi.org/10.1016/0734-189X(85)90016-7

Szegedy, C., Liu, W., Jia, Y., Sermanet, P., Reed, S., Anguelov, D., Erhan, D., Vanhoucke, V., & Rabinovich, A. (2015). Going deeper with convolutions [ISSN: 1063-6919], *07-12-June-2015*, 1–9. https://doi.org/10.1109/CVPR.2015.7298594

Szeto, G., Straker, L., & O'Sullivan, P. (2005). A comparison of symptomatic and asymptomatic office workers performing monotonous keyboard work - 2: Neck and shoulder kinematics. *Manual Therapy*, *10*(4), 281–291. https://doi.org/10.1016/j.math.2005.01.005

Toosi, K. K., Hogaboom, N. S., Oyster, M. L., & Boninger, M. L. (2015). Computer keyboarding biomechanics and acute changes in median nerve indicative of carpal tunnel syndrome. *Clinical Biomechanics*, *30*(6), 546–550. https://doi.org/10.1016/j.clinbiomech.2015.04.008

UMass Amherst. (n.d.). An Overview of Quizzes in Moodle — UMass Amherst Information Technology — UMass Amherst. Retrieved October 26, 2021, from https://www.umass.edu/it/support/moodle/overview-quizzes-moodle

Wheatland, N., Wang, Y., Song, H., Neff, M., Zordan, V., & Jörg, S. (2015). State of the Art in Hand and Finger Modeling and Animation. *Computer Graphics Forum*, *34*(2), 735–760. https://doi.org/10.1111/cgf.12595

Wu, T.-L., & Senda, T. (2021). *Pen Spinning Hand Movement Analysis Using MediaPipe Hands* (tech. rep. arXiv:2108.10716) [arXiv:2108.10716 [cs] type: article]. arXiv. https://doi.org/10.48550/arXiv.2108.10716

Yousaf, M., & Habib, H. (2014). Virtual Keyboard: Real-Time Finger Joints Tracking for Keystroke Detection and Recognition. *Arabian Journal for Science and Engineering*, *39*(2), 923–934. https://doi.org/10.1007/s13369-013-0909-2